

Low Cost Microfluidic Flowsensor

Jacky Jiang

2022-03-29

Table of Contents

1. Requirements	3
2. Verification	3
2.1. FS1 & FS2	4
2.2. FS3	7
2.3. FS4	11
2.3.1. Phosphate Buffered Saline 1x (PBS)	13
2.3.2. Phosphate Buffered Saline 10x (PBS)	15
2.3.3. Salt Water (10%)	17
2.3.4. Isopropyl Alcohol (IPA)	19
2.4. FS5	21
2.5. FS6	22
2.5.1. Cold Water (10C)	23
2.5.2. Hot Water (40C)	24
3. Flow Rate Sensor	28
3.1. Operating Theory	28
3.2. Flow Rate Sensor Hardware	29
3.2.1. Important Components	29
3.2.2. PCB Design	31
3.2.2.1. Surface Temperature Measurement Technique	33
3.2.3. Measurement Tube Design	35
3.2.3.1. Hydraulic Analysis of Measurement Tube	36
3.2.4. Cost of Flow Rate Sensor	37
3.3. Flow Rate Sensor Firmware	38
3.3.1. Analytical Model & Timedelta Extraction	38
3.3.2. Timedelta to Flow Rate Conversion	41
3.3.3. Firmware Details & Cyclic Executive	43

3.4. Manufacturing Guide	47
3.5. Calibration Guide	53
3.6. Robustness to Varying Operating Conditions	53
3.6.1. Temperature Variance	53
3.6.2. Reagent Variance	54
3.7. Known Issues & Future Improvements	54
3.7.1. PCB Self Heating	54
3.7.2. Lower Accuracy at Higher Flow Rates	55
3.7.3. High Measurement Latency	55
4. Bibliography	57
5. Appendix	58
9.1. Flow Rate Sensor	58
9.1.1. Overview of Flow Sensing Techniques	58
9.1.2. Flow Rate Sensor Prototypes	59
9.1.2.1. Prototype #1: Temperature Sensing POC	59
9.1.2.2. Prototype #2: Thermal Heating/Cooling POC	61
9.1.3. BOM Cost Estimation	65
9.1.3.1. PCB Cost	65
9.1.3.2. Electrical Components Cost	66
9.1.3.3. Mechanical Component Cost	67
6. Glossary	68
7. Changelog	70

1. Requirements

Type	#	Description	Rationale	Other Notes
F	FS1	Sensing device: An external device can read the flow rate from the sensor	Self-explanatory	
F	FS2	Measurement range: Capable of measuring flow rates up to 80 uL/min	Specified by client.	
F	FS3	Measurement uncertainty: Flow rate quantization uncertainty must be less than 10% (plus-minus 10% with respect to measurement taken)	Specified by client.	
NF	FS4	Reagent compatibility: Supports the measurement of many different reagents without manual intervention	Multiple reagents will be used over the course of a single experiment	
NF	FS5	Insensitivity to ambient temperature variations: Sensor accuracy is not sensitive to the ambient air temperature	Ambient air temperature changes throughout the day and the year. The performance of the sensor should not be greatly affected	
NF	FS6	Insensitivity to reagent temperature variations: Sensor accuracy is not sensitive to the reagent temperature	Reagents will have different temperatures depending on the situation. The performance of the sensor should be relatively similar	

2. Verification

We verified that all flow sensing requirements passed except FS5, whose verification is skipped.

Our goal was to give a first order characterization and qualification of our low cost flowsensor. The metrics we use are insightful but crude. For better qualification, consult the National Institute of Standards and Technology (NIST) Engineering Statistic Handbook at <https://www.itl.nist.gov/div898/handbook/index.htm>.

2.1. FS1 & FS2

Life Science Institute (LSI) Lab at the University of British Columbia (UBC) has a fluigent microfluidic dispensing system.

They can dispense reagents at set regulated flow rates. The flowsensor used in this system is the Sensirion SLI-0430 FMK flowsensor.

We connect our low cost flow sensor in-series with SLI-0430. We assume that the fluigent system is regulating the flow rate perfectly, which allows us to record only the output of our low cost flow sensor.

Here's the result of our benchmarking with distilled, deionized water (DDW).

Sensirion SLI-0430 vs Low Cost Flowsensor

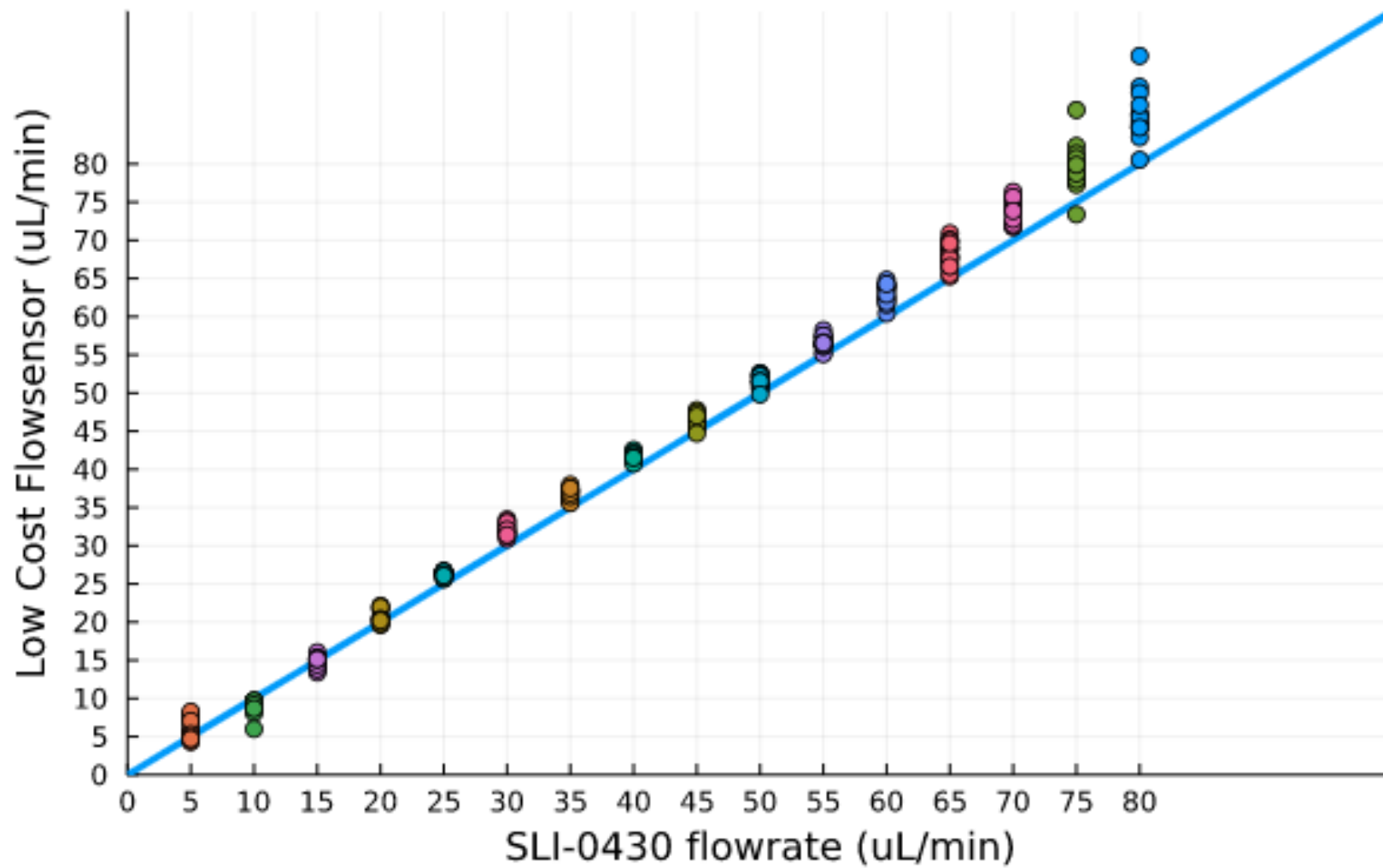


Figure 2.1. Low cost flowsensor measurements at set flow rates

We took at least 12 measurements at each flow rate starting from 5 $\mu\text{L}/\text{min}$ to 80 $\mu\text{L}/\text{min}$ at increments of 5 $\mu\text{L}/\text{min}$. If the measurements were perfect, then they would all fall on the blue line. As we can see, the flow rate measurements of the low cost flowsensor correspond fairly well to the reference flow rate. The error does increase as we enter the higher flow rate regions.

Based on this data, we successfully validated that the sensor is capable of measuring flow rates up to 80 $\mu\text{L}/\text{min}$ (FS2) and that it can offload the data to an external device (FS1).

2.2. FS3

We decided to characterize the accuracy of our sensor by using the median accuracy in %of measured value (%of m.v.) . We also provide results for accuracy in %of full scale (%of f.s.).

To show the distinction between %of m.v. and %of f.s., consider the following example. If we measure a flow rate that is set to 20 uL/min, and the flowsensor has 10%of m.v., this means that the uncertainty is $10\% * 20 \text{ uL/min} = 2\text{uL/min}$. Our measurement of a 20 uL/min flow rate can be anything between 18 and 22 uL/min.

If instead, the accuracy is 10%of f.s., then the the uncertainty is $10\% * \text{full scale}$. The full scale for our sensor is 80 uL/min. Our uncertainty at any flow rate is then 8 uL/min. Our measurement of a 20 uL/min flow rate can be anything from 12 to 28 uL/min.

We also chose to use the median of the accuracy. We believe that the median is the most useful statistical quantity as a first order qualification of our sensor. Whenever we take a measurement, then the accuracy of that measurement is most likely to be the median accuracy by the definition of the median. Note that this means that there will be measurements with lower accuracies than the accuracy used to qualify our sensor.

Using the same benchmarking data collected from the LSI lab from section 6.4.1., we perform the following measurement uncertainty analysis.

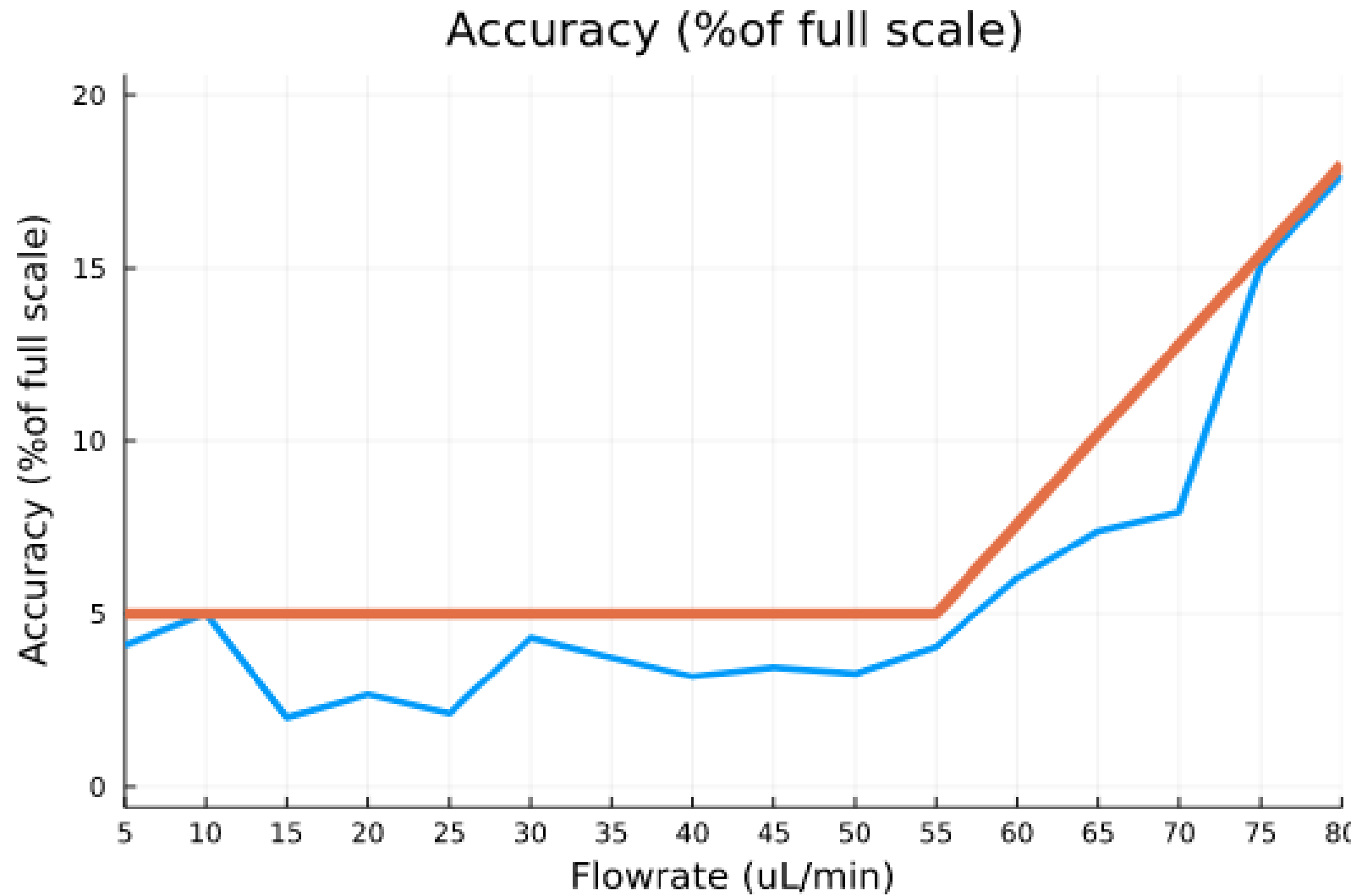


Figure 2.2. The blue line is the uncertainty from the benchmarking data.

The orange line is an error upper bound to communicate sensor accuracy expectations through the product specification sheet

As seen in figure 2.2, the absolute error below 60 uL/min is only 5 uL/min. However, this error increases linearly as the flow rate is set beyond 60 uL/min. Following datasheet conventions, we provide an error upper bound for the product specification sheet.

We can confidently say that the accuracy below 55 uL/min is 5% of full scale and that the accuracy below 80 uL/min is below 18% of full scale.

Here is the characterization of the accuracy in %of m.v.

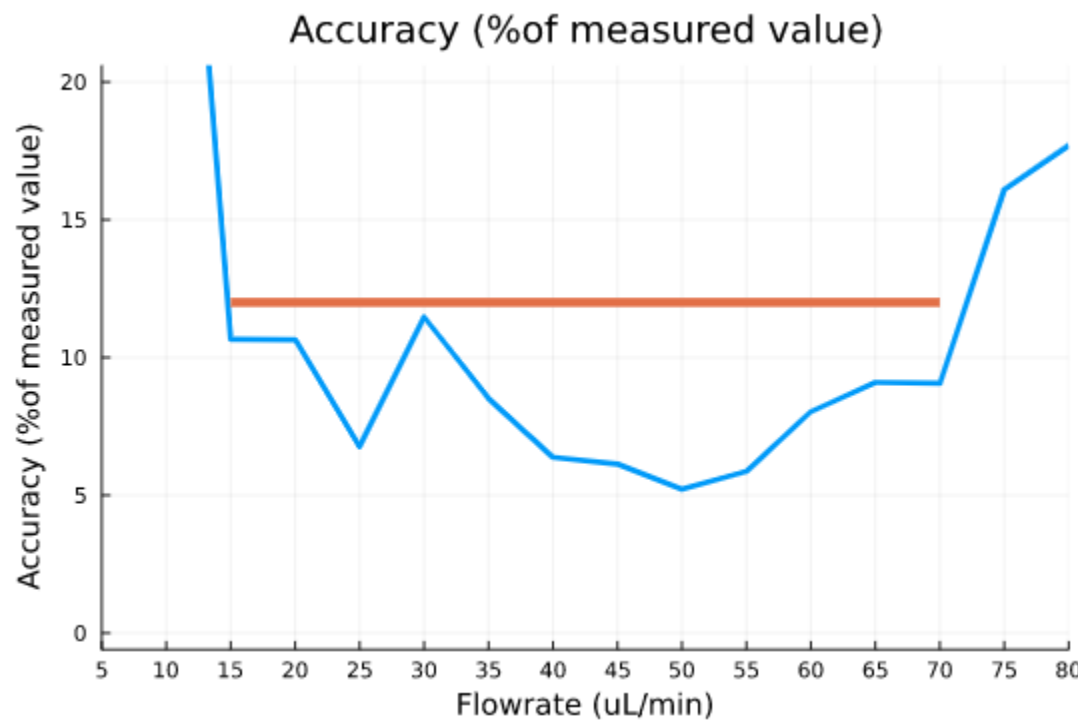


Figure 2.3. The blue line is the uncertainty from the benchmarking data.

The orange line is an error upper bound to communicate sensor accuracy expectations through the product specification sheet

Here, we see that the accuracy in %of m.v. is at or below 12% between 15 uL/min and 70 uL/min. It increases at the higher flow rate region but stays below 18%.

The error also increases at the lower flow rate region. This is due to the self-heating problem discussed in the design document. The absolute accuracy is still good. For example, 50% accuracy while measuring 5 uL/min is still only 2.5 uL/min.

	variable	mean	min	median	max	nmissing	eltype
1	:abs_err	4.5975	1.6	3.25	14.15	0	Float32
2	:measurement_err	14.8148	5.22	9.08187	65.4	0	Float32
3	:fullscale_err	5.74687	2.0	4.0625	17.6875	0	Float32
4	:flow	42.5	5	42.5	80	0	Int32

Figure 2.4. Statistical summary of measurement uncertainty:

abs_err: absolute measurement uncertainty is uL/min

measurement_err: accuracy in %of m.v.

fullscale_err: accuracy in %of f.s.

flow: flow rates

FS3 demands that the accuracy of the sensor be 10% of m.v.

According to figure 2.4, the median accuracy (%of m.v.) is 9.1%, which satisfies the accuracy requirement. As such, the FS3 requirement is satisfied as we use the median accuracy to characterize our sensor. However, keep in mind that measurements at below 15 uL/min or above 70 uL/min flow rates are consistently higher than 10% of m.v.

2.3. FS4

To demonstrate reagent compatibility, we will collect verification data for the following list of common reagents.

1. 1x Phosphate-buffered Saline (PBS)
2. 10x Phosphate-buffered Saline
3. Salt Water (10% Concentration)
4. Isopropyl Alcohol (IPA)

We will be using a syringe pump to collect the data. Since the sensor that underwent FS2 verification was calibrated on data collected from this syringe pump, we know that its accuracy is sufficient for our purposes.

We run the same analysis as before on these new reagents. We summarize the results below.

Reagent	Median Accuracy (% of m.v.)	Median Accuracy (% of f.s.)
DDW (from FS2)	9	4
1x PBS	12	5
10x PBS	11	6
Salt Water (10%)	10	4

Figure 2.5. A summary table displaying the median accuracy for a variety of reagents

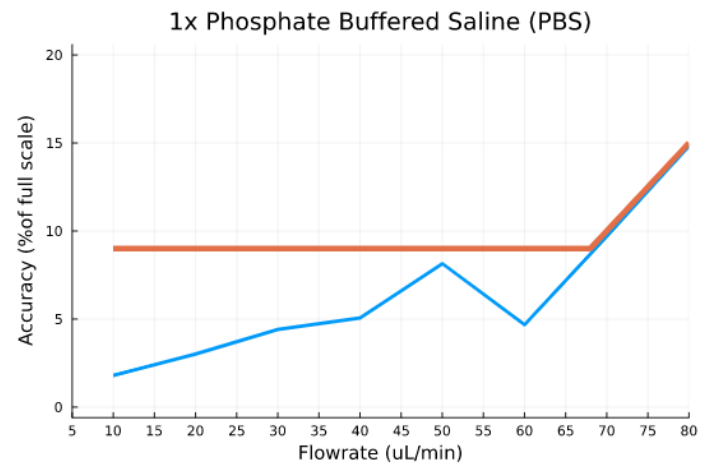
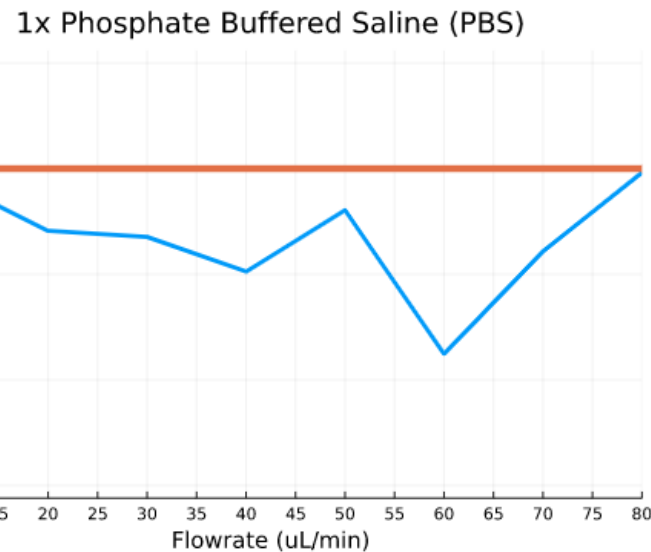
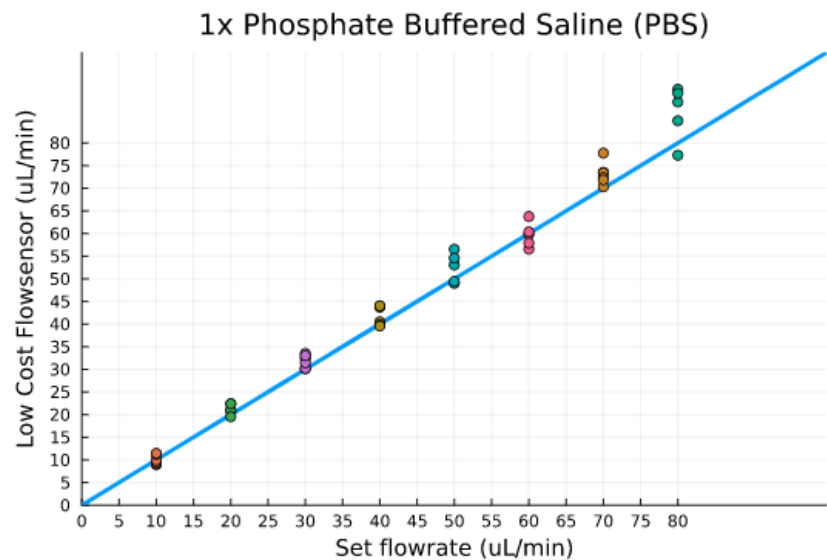
In other words, all reagents except IPA can be measured fairly accurately with the flowsensor. The salt water measurement accuracy is comparable to DDW whereas the 1x and 10x PBS accuracy (% of m.v.) is around 3% worse.

We expected the IPA flow rate measurement accuracy to be inaccurate because a similar phenomenon is noted in the datasheet of our client's off-the-shelf flowsensor (SLI-0430). As such, we are not including IPA as part of the requirements to pass FS4.

Since all other tested reagents yielded comparable results to DDW, we conclude that the flowsensor can measure the flow rate of a variety of reagents without manual intervention. Hence we pass the FS4 requirement. However, it is important to note that some of these reagents push the median accuracy above 10% of m.v., which is below FS3 accuracy requirements.

2.3.1. Phosphate Buffered Saline 1x (PBS)

The 1x PBS was given to us by our client. It was taken from the LSI Lab.



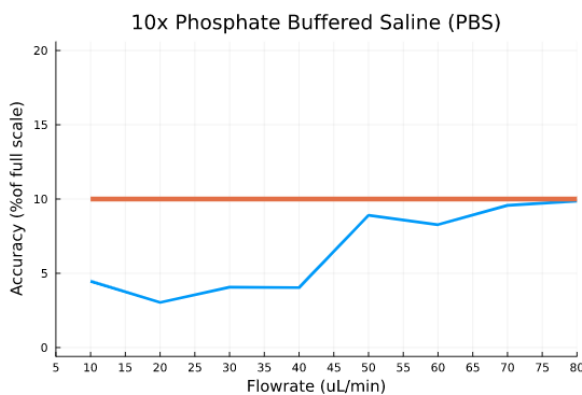
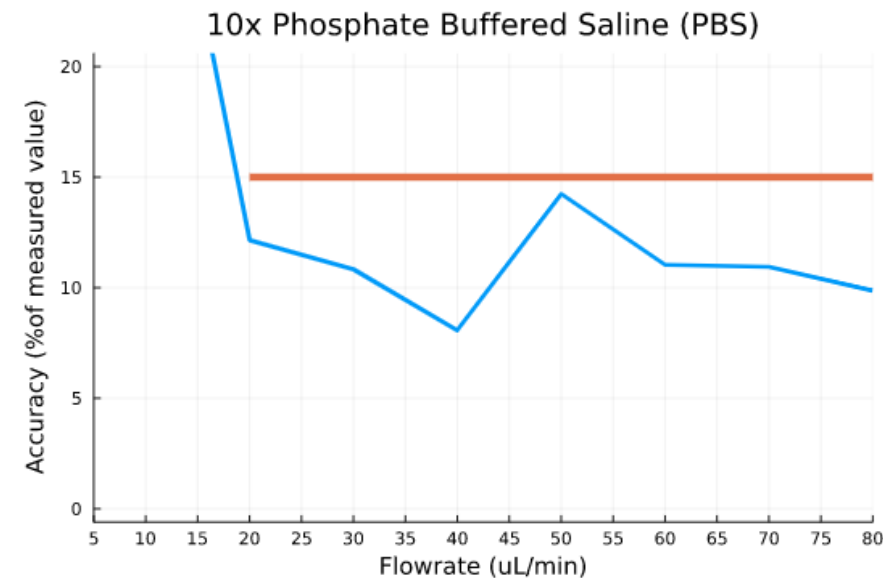
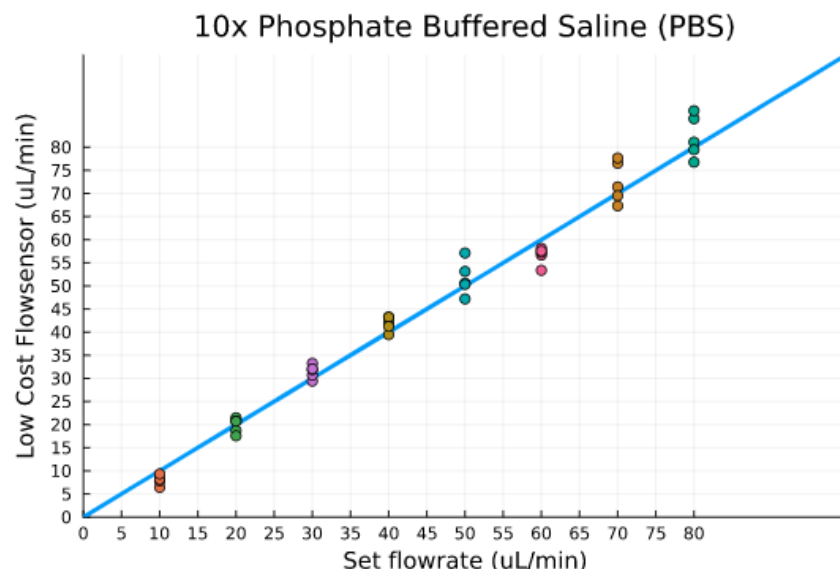
variable	mean	min	median	max	nmissing	eltype
1 :abs_err	5.1625	1.44	3.895	11.85	0	Float32
2 :measurement_err	11.6892	6.23334	11.9083	14.8125	0	Float32
3 :fullscale_err	6.45312	1.8	4.86875	14.8125	0	Float32
4 :flow	45.0	10	45.0	80	0	Int32

Figure 2.6. Experimental results for 1x PBS consisting of flowsensor outputs vs set flow rates (top left), a statistical summary of measurement uncertainty (bottom right), accuracy in %of m.v. (top right) and accuracy in %of f.s. (bottom left)

The flow rate accuracy is around 3% of m.v. worse than regular water.

2.3.2. Phosphate Buffered Saline 10x (PBS)

The 10x PBS was given to us by our client. It was taken from the LSI Lab.



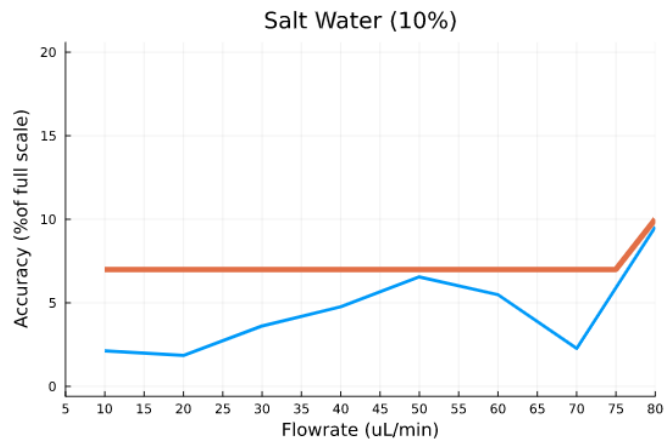
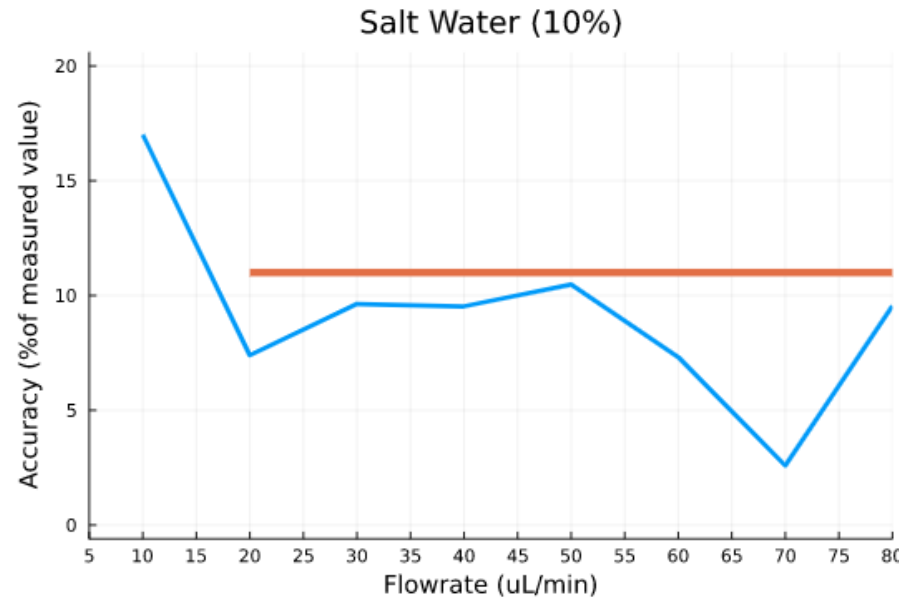
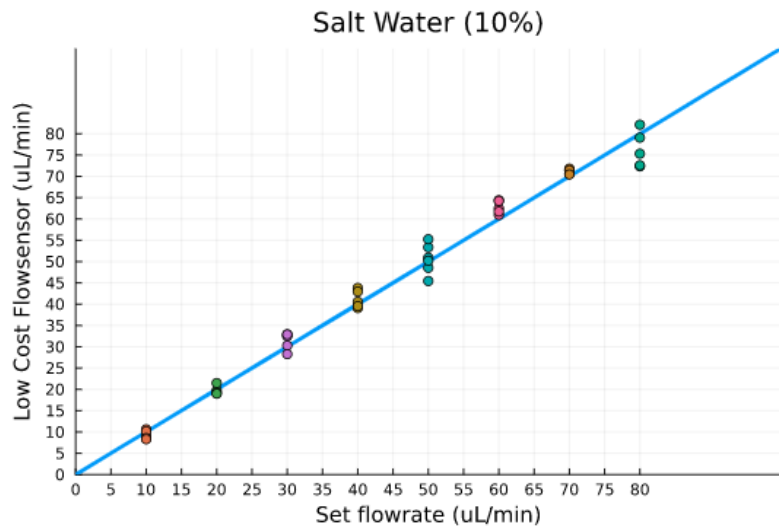
variable	mean	min	median	max	nmissing	eltype
1 :abs_err	5.22125	2.43	5.095	7.89	0	Float32
2 :measurement_err	14.1046	8.075	10.9881	35.7	0	Float32
3 :fullscale_err	6.52656	3.0375	6.36875	9.8625	0	Float32
4 :flow	45.0	10	45.0	80	0	Int32

Figure 2.7. Experimental results for 10x PBS consisting of flowsensor outputs vs set flow rates (top left), a statistical summary of measurement uncertainty (bottom right), accuracy in %of m.v. (top right) and accuracy in %of f.s. (bottom left)

Has comparable accuracy to 1x PBS.

2.3.3. Salt Water (10%)

The salt water (saline) solution was made by mixing 1 tablespoon of salt and 9 tablespoons of water at room temperature.



variable	mean	min	median	max	nmissing	eltype
1 :abs_err	3.62	1.48	3.35	7.64	0	Float32
2 :measurement_err	9.18634	2.58571	9.5375	17.0	0	Float32
3 :fullscale_err	4.525	1.85	4.1875	9.55	0	Float32
4 :flow	45.0	10	45.0	80	0	Int32

Figure 2.8. Experimental results for salt water (10% concentration) consisting of flowsensor outputs vs set flow rates (top left), a statistical summary of measurement uncertainty (bottom right), accuracy in %of m.v. (top right) and accuracy in %of f.s. (bottom left)

Has the same performance as regular water.

2.3.4. Isopropyl Alcohol (IPA)

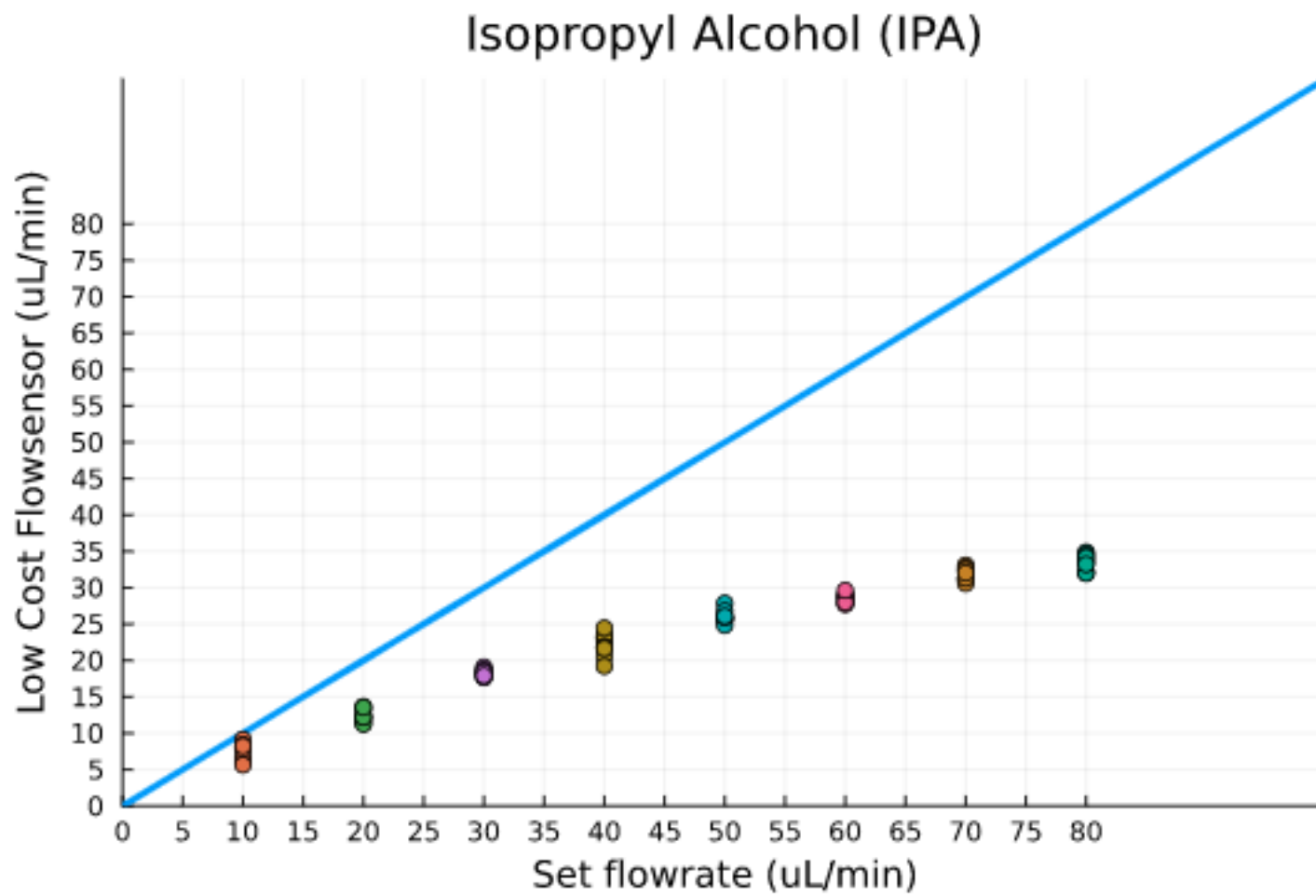


Figure 2.9. Flowsensor outputs vs set flow rates for IPA

The error analysis is not very useful here because we clearly see that the measurement accuracy is poor. The sensor must be recalibrated specifically to measure IPA.

2.4. FS5

We decided to skip verification for FS5 for a few reasons.

Firstly, we assume that this sensor will be used in a temperature regulated room. We do not expect ambient temperature to deviate much from standard room temperatures.

Secondly, as discussed in the design document, we have strong reasons to expect that changes in the ambient temperature will not greatly affect the accuracy of the sensor.

Thirdly, altering the ambient temperature around the entire experiment is a difficult process and it would take time to secure the equipment required to perform such a verification. This time is better spent elsewhere to enhance the system as a whole.

Lastly, there are only two ways for the ambient temperature to affect the measurement. One way is that it alters the amount of heat transfer from the heater to the reagent and from the reagent to the environment. The other way is that it will slightly change the mechanical properties of the sensor.

We believe both effects can be simulated by altering the reagent temperature, which is much easier to do than altering the ambient temperature. Since we are verifying that the sensor accuracy is invariant with reagent temperature for FS6, we decided that it would be alright to skip FS5 verification. The results from FS6 verification should be a good proxy result which would hint at how accuracy changes with changing ambient temperatures.

2.5. FS6

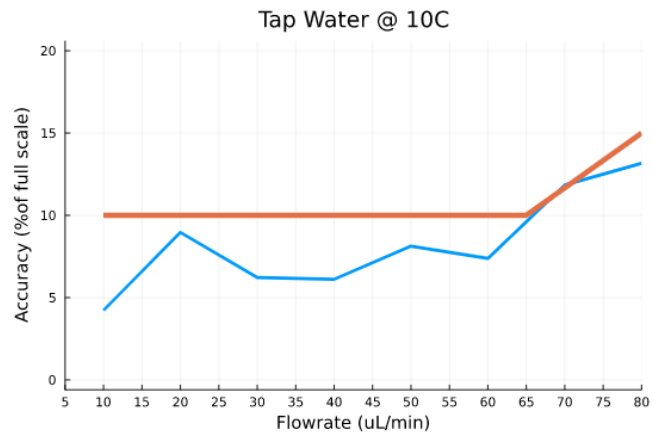
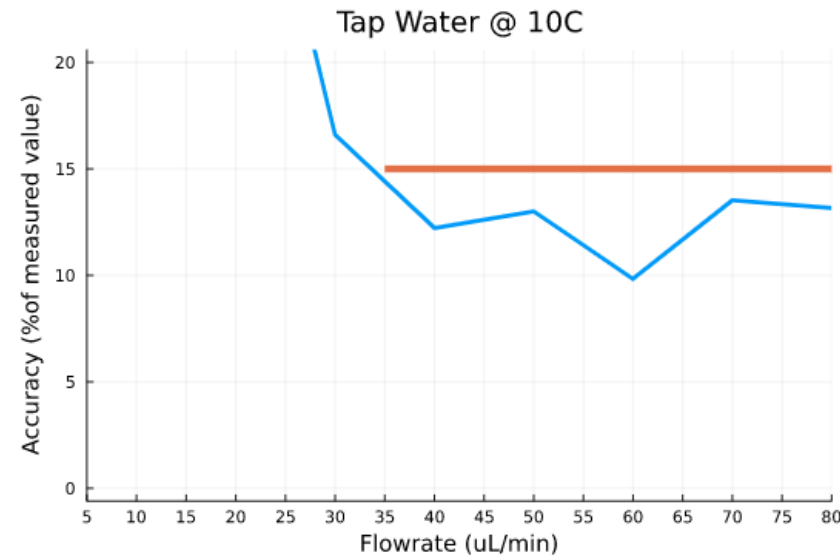
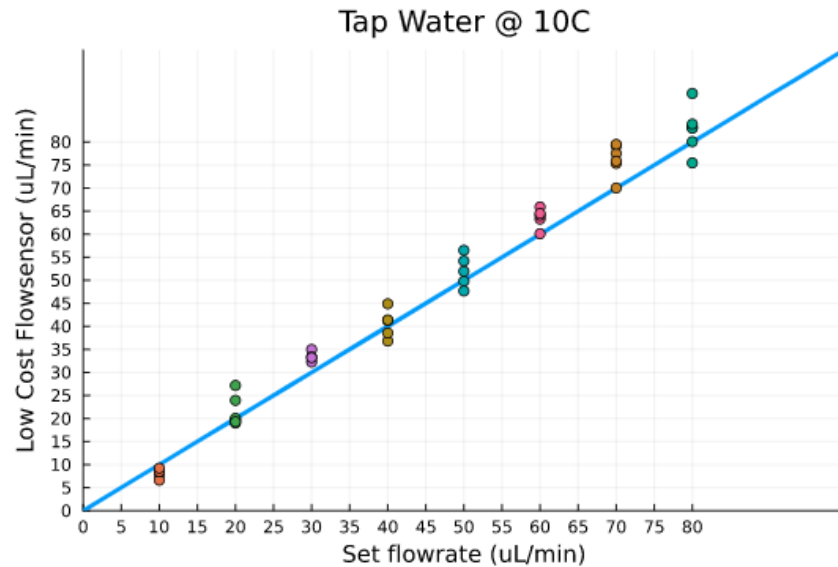
Sensor accuracy should not be sensitive to reagent temperature. For this verification test, we collect flow rate measurements of cold tap water at 10C and hot tap water at 40C.

We found that the flowsensor was about 5%of m.v. less accurate when measuring cold and hot water than when measuring water at room temperature.

A deviation this small is to be expected as the sensor was calibrated at room temperature. Since the accuracy was not affected too drastically by these extreme reagent temperatures, we passed the FS6 requirement. However, as with FS4, the differing temperatures does push the median accuracy in %of m.v. over the accuracy requirement of FS3.

2.5.1. Cold Water (10C)

Cold water was taken from the sink. A thermometer is used to ensure the temperature of the water stays at or below 10C. Whenever the temperature of the water is heated to above 10C, that water is replaced with colder water from the sink.



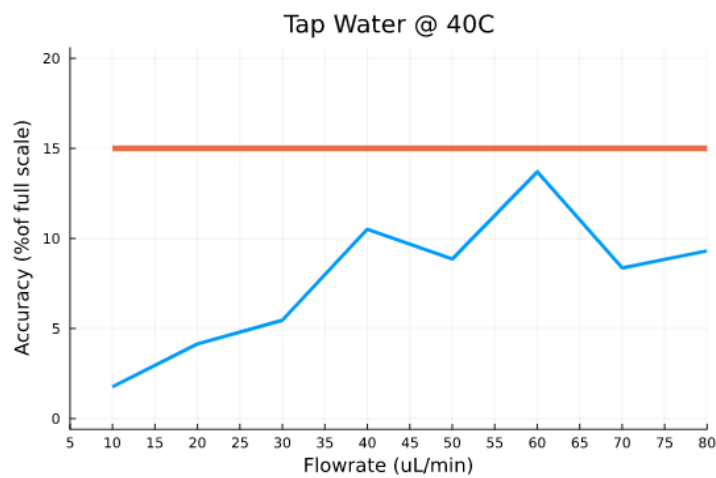
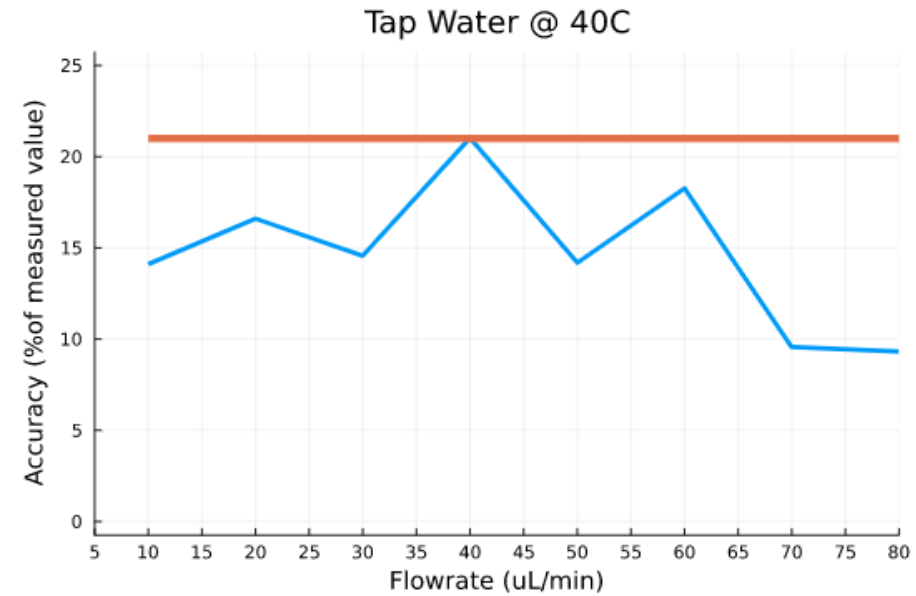
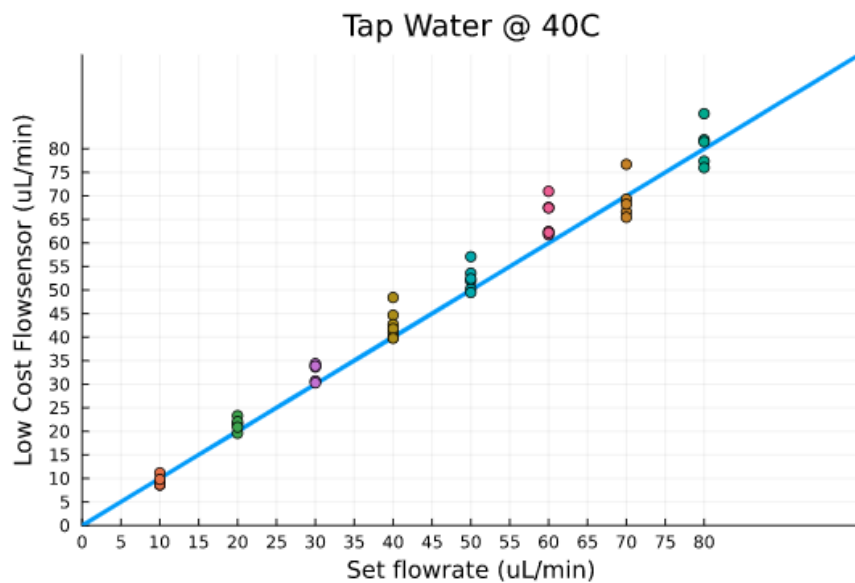
variable	mean	min	median	max	nmissing	eltype
1 :abs_err	6.6025	3.38	6.2	10.53	0	Float32
2 :measurement_err	18.4999	9.83334	13.3455	35.85	0	Float32
3 :fullscale_err	8.25313	4.225	7.75	13.1625	0	Float32
4 :flow	45.0	10	45.0	80	0	Int32

Figure 2.10. Experimental results for cold water (10C) consisting of flowsensor outputs vs set flow rates (top), a statistical summary of measurement uncertainty (middle), accuracy in %of m.v. (bottom left) and accuracy in %of f.s. (bottom right)

Cold water at 10C has 4% of m.v. more uncertainty than water at room temperature.

2.5.2. Hot Water (40C)

Hot water was taken from the sink. A thermometer is used to ensure the temperature of the water stays at or above 40C. Whenever the temperature of the water is cooled to below 40C, that water is replaced with hotter water from the sink.



	variable	mean	min	median	max	nmissing	eltype
1	:abs_err	6.2125	1.41	6.89	10.96	0	Float32
2	:measurement_err	14.701	9.3125	14.3733	21.025	0	Float32
3	:fullscale_err	7.76562	1.7625	8.6125	13.7	0	Float32
4	:flow	45.0	10	45.0	80	0	Int32

Figure 2.11. Experimental results for hot water (40C) consisting of flowsensor outputs vs set flow rates (top), a statistical summary of measurement uncertainty (middle), accuracy in %of m.v. (bottom left) and accuracy in %of f.s. (bottom right)

Hot water at 40C has 5%of m.v. more uncertainty than water at room temperature.

3. Flow Rate Sensor

3.1. Operating Theory

The flow rate sensor employs the thermal, time-of-flight sensing technique. A temperature sensor is placed downstream of a heater. The heater provides a heat pulse which increases the temperature of the fluid in the region around it. If there is flow, then the heated fluid flows towards the temperature sensor where the higher temperature is detected. The delay between heating the fluid and sensing the increased temperature is used to determine the volumetric flow rate.

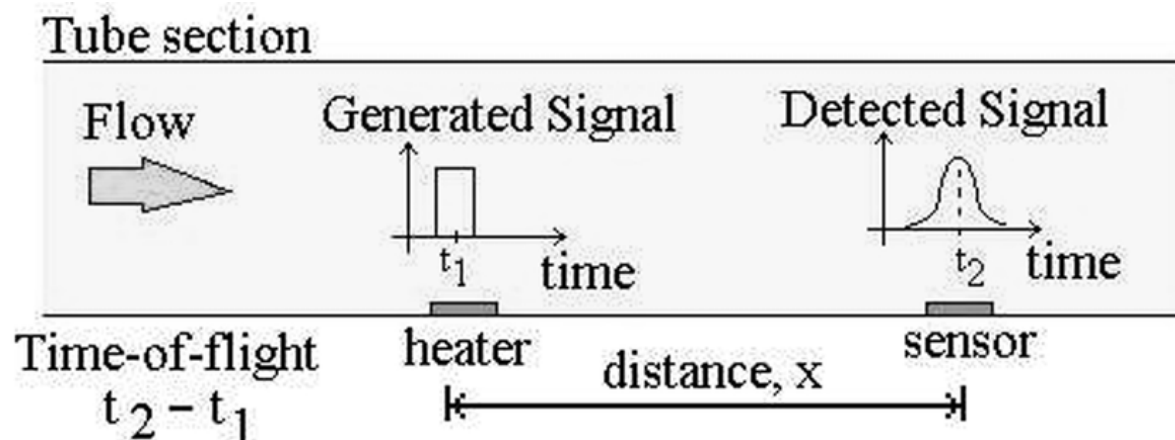


Figure 3.1: Diagram displays thermal time-of-flight operating theory [1]

Typically, another temperature sensor is placed upstream to record the temperature of the fluid before the fluid gets heated.

This method is chosen over another popular method called the calorimetric measuring method. In the calorimetric measuring method, heat is constantly applied to the reagent, and the flow rate is detected by measuring the heat displacement. This method is far more complicated than the time-of-flight method which is why we chose not to pursue the calorimetric measuring method.

3.2. Flow Rate Sensor Hardware

First we describe the important components used in the construction of the sensor.

Next we give an overview of the sensor PCB and the functions it performs. We pay special attention to how the temperature sensing is done, as it dictates important characteristics of the PCB such as its thinness, its conductive-filled vias, and its hard-gold finish.

Next, we shift focus to discuss how the measurement tube was made and estimate its hydraulic resistance as well as its dead volume.

Finally we provide a comprehensive estimate of the BOM cost at 500 units.

3.2.1. Important Components

The function of each component should follow directly from the operating theory described in section 3.1, but a brief description of each component is given to solidify the connection and provide greater detail.

Functional Name	Component Name	Important Parameters
Stainless Steel Tube	<u>Easy Touch Bag of 20 1cc 29 1/2 inch 100 units</u>	High thermal conductivity
Resistive Heater Wire	<u>0.1mm AWG38 Nichrome Resistance</u>	138.8Ohm/M

	<u>Heating Coils Resistor Wire</u>	
Thermally Conductive, Electrically Insulative Epoxy	<u>MG Chemicals 8329TCM-6ML Thermal Conductive Adhesive</u>	1.4 W/(m·K)
High Precision Temperature Sensors	<u>TMP117</u>	+0.1C Accurate [3]
Soft-walled Microfluidic Tubing	<u>Tygon Microbore tubing, 0.010" x 0.030"OD, 100 ft/roll</u>	0.01" ID

Table 3.1: List of important components

Stainless Steel Tube: A thermally conductive material must be used to carry thermal energy from the heater to the fluid and from the fluid to the temperature sensor. Stainless steel tubing is chosen for this role. They are mechanically robust, resists oxidation and most importantly, are already a common material used in microfluidic projects. For example, researchers often use syringes equipped with a stainless steel tube to drive flow to and from microfluidic chips.

Resistive Heater Wire: This type of wire is typically used in heating applications. They can be wound around the stainless steel tube, thereby using the full surface area for fast heat transfer.

Thermally Conductive, Electrically Insulative Epoxy: Used to electrically insulate the resistive wire and the temperature sensor from the stainless steel tubing while allowing for heat transfer between them.

High Precision Temperature Sensors: Catches the increased thermal energy for time-of-flight measurements.

Soft-walled Microfluidic Tubing: The tubing must be soft-walled so that the stainless steel tubing can directly connect without any additional adapters. In section 3.2.3, it is clear that the distances required between the heating and sensing section precludes the use of any adapters.

3.2.2. PCB Design

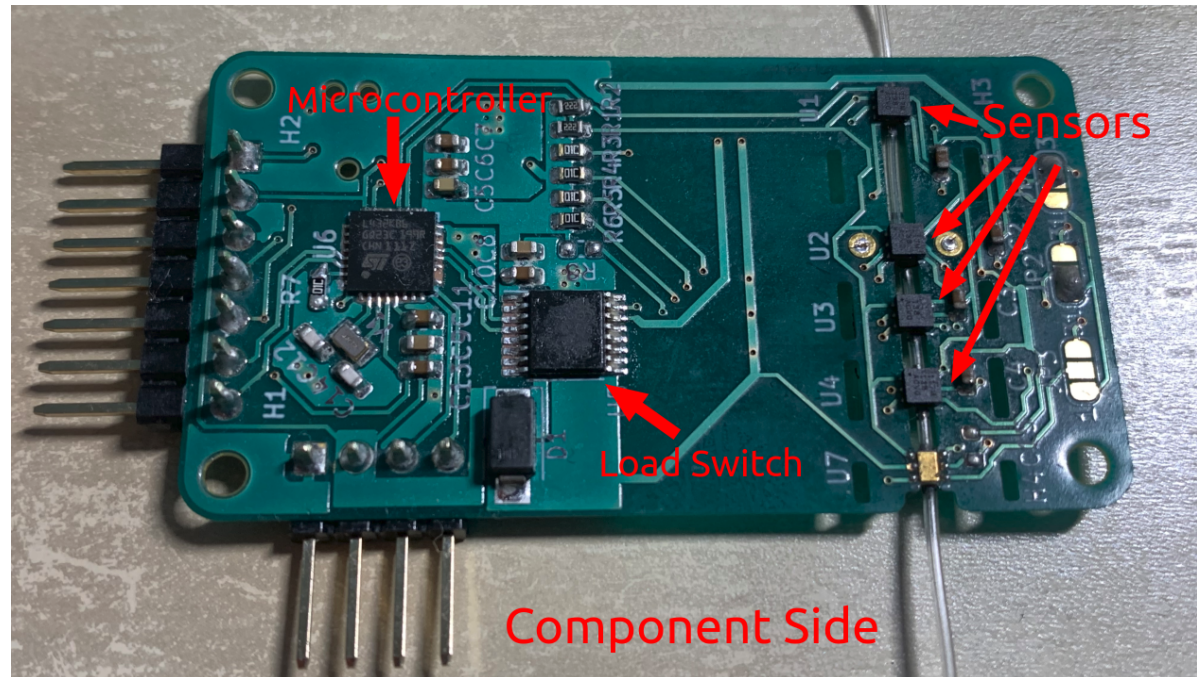


Figure 3.2: Component side of the flow rate sensor with important components highlighted

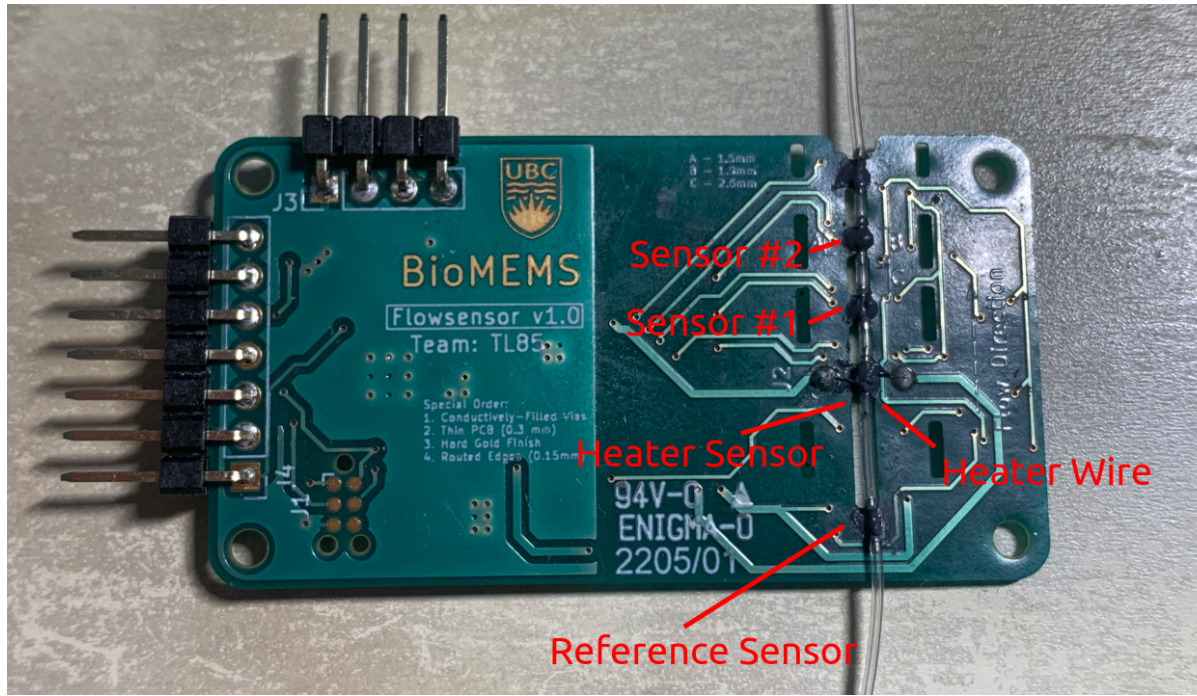


Figure 3.3: Measurement side of the flow rate sensor with important components highlighted

The PCB contains a STM32L432KB microcontroller which reads 4 TMP117 temperature sensors. It also contains a load switch which controls the power applied to the heater.

Reference sensor measures the temperature of the fluid before the heater.

Heater sensor verifies that the heater does not rise above body temperature (37 C), which is the temperature where proteins begin to denature.

Sensor #1 is the first sensor downstream of the heater. It accurately measures low flow rates.

Sensor #2 is the second sensor downstream of the heater. It accurately measures high flow rates.

The STM32L432KB is responsible for operating the heater, reading temperature data from the TMP117 sensors, converting the temperature data to a flow rate value and printing the flow rate value on the STM32L432KB UART pins. This satisfies FS1.

3.2.2.1. Surface Temperature Measurement Technique

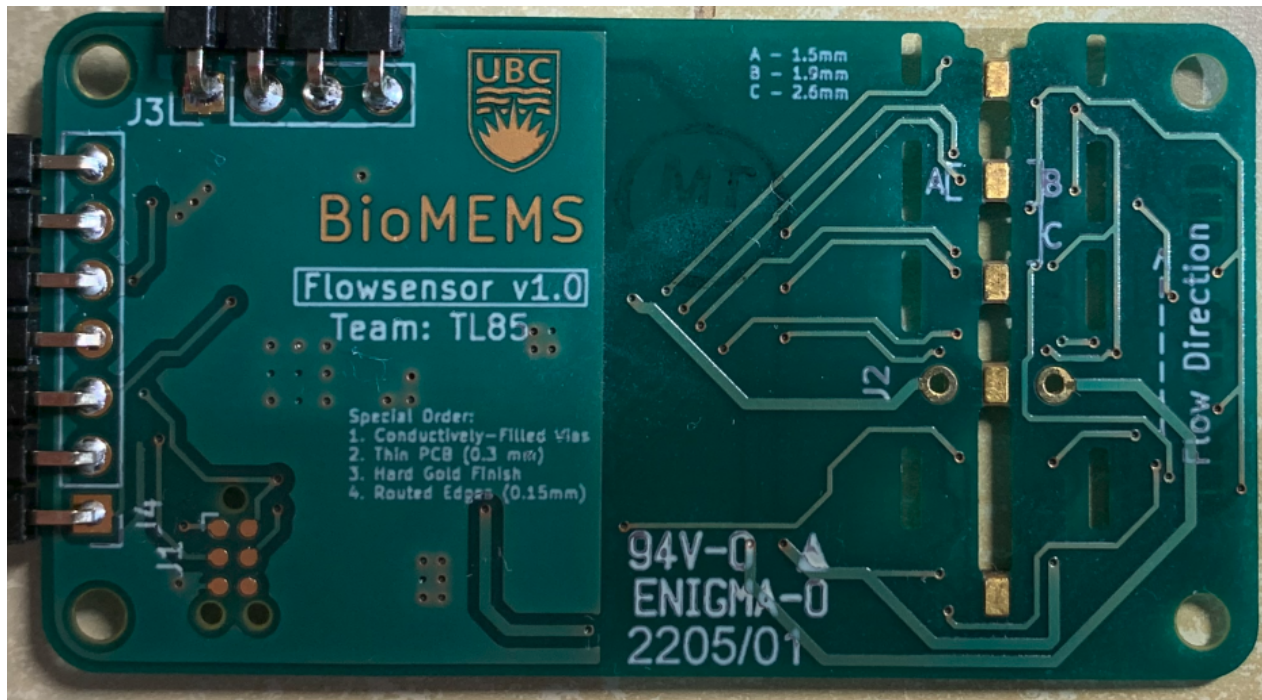


Figure 3.4: Flow rate sensor PCB before installing the measurement tube. Notice the hard gold plating and the conductive-filled vias on the “sensing pads”

Following Texas Instruments Application Report SNOA986A [4], we use the TMP117 in the way shown in figure 3.5.

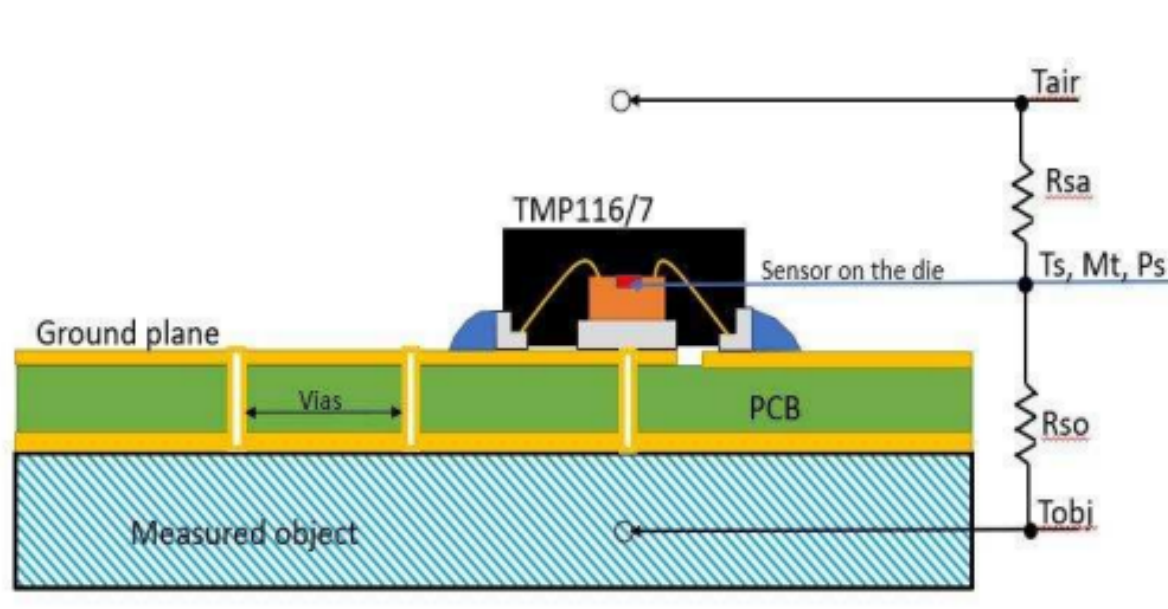


Figure 3.5: The measured object imparts thermal energy to the bottom side of the PCB. That thermal energy is carried through the vias to the TMP117 sensor mounted on the top side of the PCB

To minimize thermal resistance, the PCB is only 0.3 mm thick. There are also 6 thermal vias connecting each of the TMP117 thermal pads to the “sensing pads” located at the bottom of the PCB. These vias are conductively filled to further decrease thermal resistance.

3.2.3. Measurement Tube Design

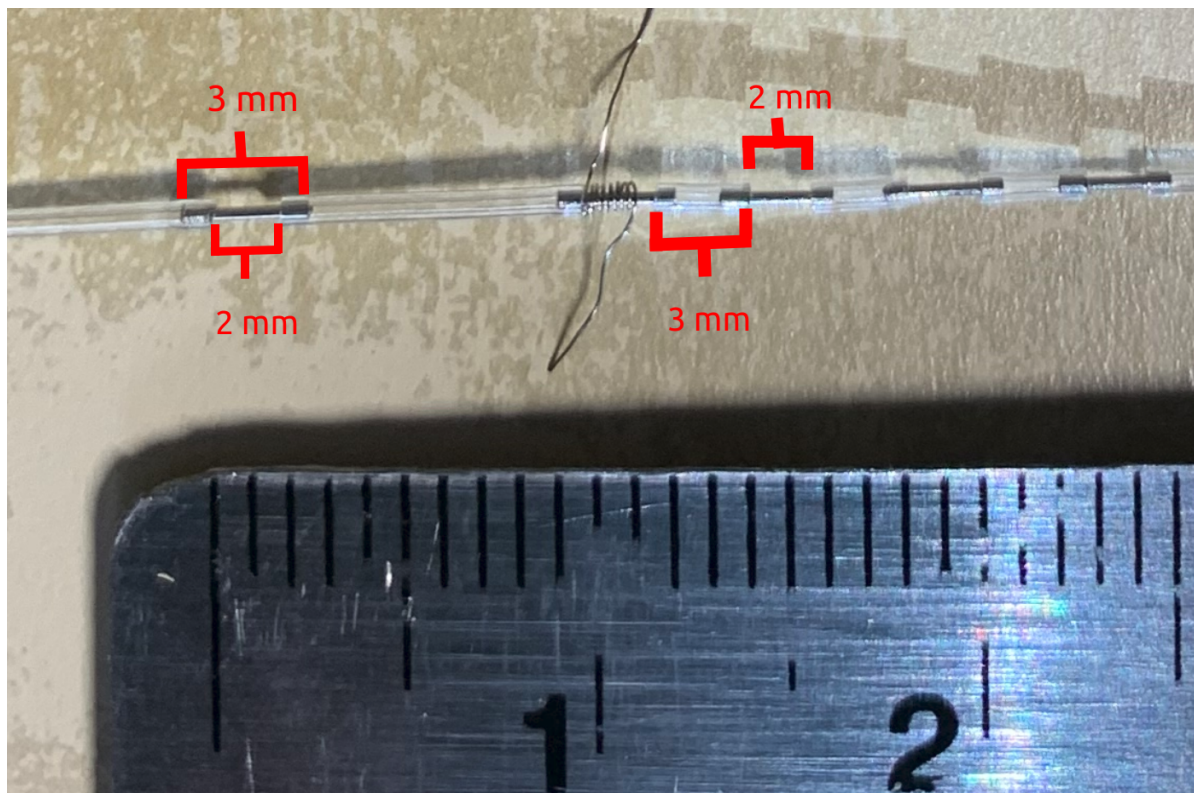


Figure 3.6: Measurement Tube. The coil of wire around the second stainless steel section is the heater wire.

We use 0.01' ID tygon tubing as the main tubing because it is soft-walled, which means it can interface with the stainless steel tube sections directly. The dimensions of the different sections alternate between 3 mm of tygon tubing and 2 mm of exposed stainless steel tubing.

There are 3 stainless steel tubing sections downstream of the heater for possible temperature sensing locations. There is also a stainless steel tubing section upstream of the heater to measure the reference temperature before heating. Lastly, there is a stainless steel tubing section at the heater for the heater wire to transfer heat to the fluid.

The stainless steel tubes are cut from 29 gauge syringe needles. Thermally conductive epoxy is used to attach the measurement tube to the pcb at the sensing pads.

3.2.3.1. Hydraulic Analysis of Measurement Tube

Hydraulic resistance for a circular cross-section is approximately

$$R_h = \frac{8\mu L}{\pi r^4}$$

Where μ is the dynamic viscosity of the fluid. L is the length of the tubing and r is the radius of the tube.

29 gauge stainless steel needles have 0.184 mm ID. There's roughly 15 mm of stainless steel tubing and around 15 mm of tygon tubing that is actually required for the sensor. We estimate that the hydraulic resistance of the flow rate sensor to be 777928 mPa*s/mm^3

To calculate the pressure resulting from the hydraulic resistance and flow rate, we use the following relation:

$$\Delta P = Q \times R_h$$

Where P is the pressure difference, Q is the flow rate and R is the hydraulic resistance. In accordance with FS2, the maximum flow rate is 80 uL/min. Using the maximum flow rate, we find that the pressure difference is 0.01 bars.

At 80 $\mu\text{L}/\text{min}$, we only require 0.01 bars of pressure to drive the sensor.

For the dead volume, we use the same estimations above.

$$V_{dead} = 15\text{mm} * \pi * ((0.092\text{mm})^2 + (0.127\text{mm})^2) = 1.16 \mu\text{L}$$

3.2.4. Cost of Flow Rate Sensor

Component	Cost (CAD)
PCB	1.02
Electrical Components	23.64
Thermally Conductive Adhesive	2
29 Gauge Syringe Needles	0.54
0.01 ID Tygon Tubing	0.56
Nichrome Heater Wire	0.03
Total BOM Cost	27.79

Table 3.2: Breakdown of the BOM cost for the flow rate sensor

When manufacturing flow rate sensors in batches of 500, the BOM cost per sensor is only 27.53CAD. See Appendix 8.1.3. for the details of the breakdown with proof.

3.3. Flow Rate Sensor Firmware

3.3.1. Analytical Model & Timedelta Extraction

On a 100ms heating and 13000ms cooling cycle, we get the following temperature data points.

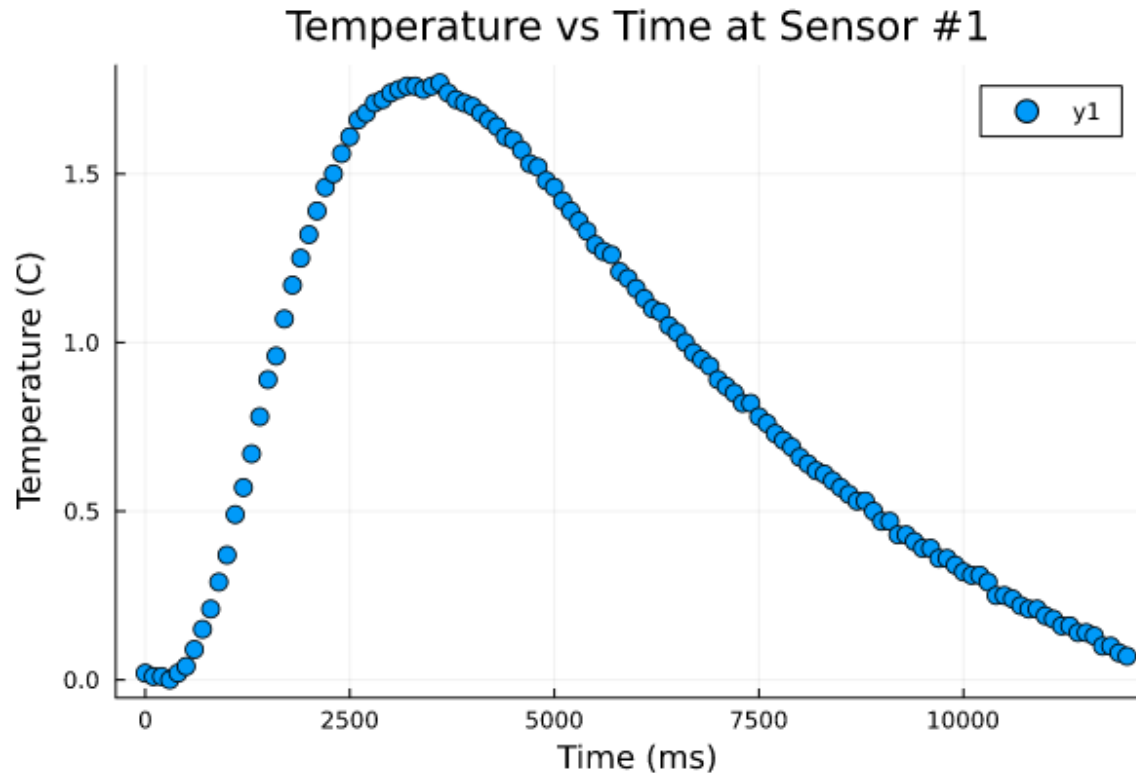


Figure 3.7: Temperature data captured at sensor #1 following a 100 ms heat pulse. The data is normalized. This particular temperature curve corresponds to a flow rate of 40 uL/min

We use the analytical model presented by Jonathon et al. [2] as a starting point. After introducing a time delay factor, we found that it fits our normalized temperature data very well.

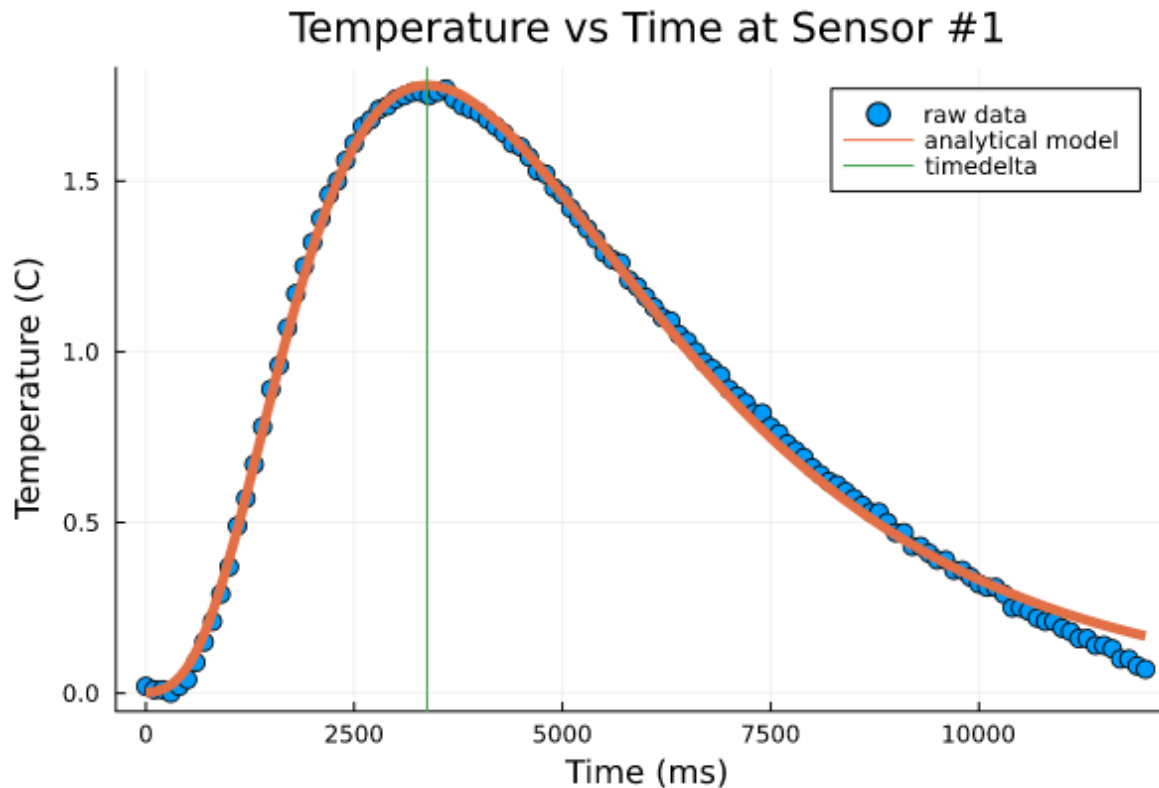


Figure 3.8: The raw data with the analytical model overlaid. Timedelta is the time between the end of the heat pulse to the peak of the temperature curve.

Once we have the parameters for our analytical model, then we can solve for the timedelta.

Our analytical model is:

$$f(t) = \frac{q}{4\pi k(t+d)} e^{-\frac{(x-v(t+d))^2}{4a(t+d)}}$$

q is the pulse signal input strength

x is the distance between the heater and the sensor in mm)

k is the thermal conductivity in w/(mm*K)

a is the thermal diffusivity in mm^2/ms

v is the average flow velocity in mm/ms

t is time (ms)

We also introduce a delay factor d to control when $t = 0$

It is important to note that since we are treating k and a as parameters, there is no need to change sensing configurations for different kinds of reagents, which is in accordance with FS4.

Furthermore, it is clear from the analytical model that the timedelta is not sensitive to the absolute temperatures involved. This makes the sensor reliable in different ambient temperatures and different fluid temperatures. This is in accordance with FS5 and FS6.

To calculate the timedelta, we use the following equation.

$$\tau = \frac{-2a + \sqrt{4a^2 + v^2x^2}}{v^2} - d$$

3.3.2. Timedelta to Flow Rate Conversion

After collecting the timedelta for a variety of flow rates spanning 5 uL/min to 80 uL/min (FS2), we plot the data on a timedelta vs flow rate graph and fit a decaying exponential function.

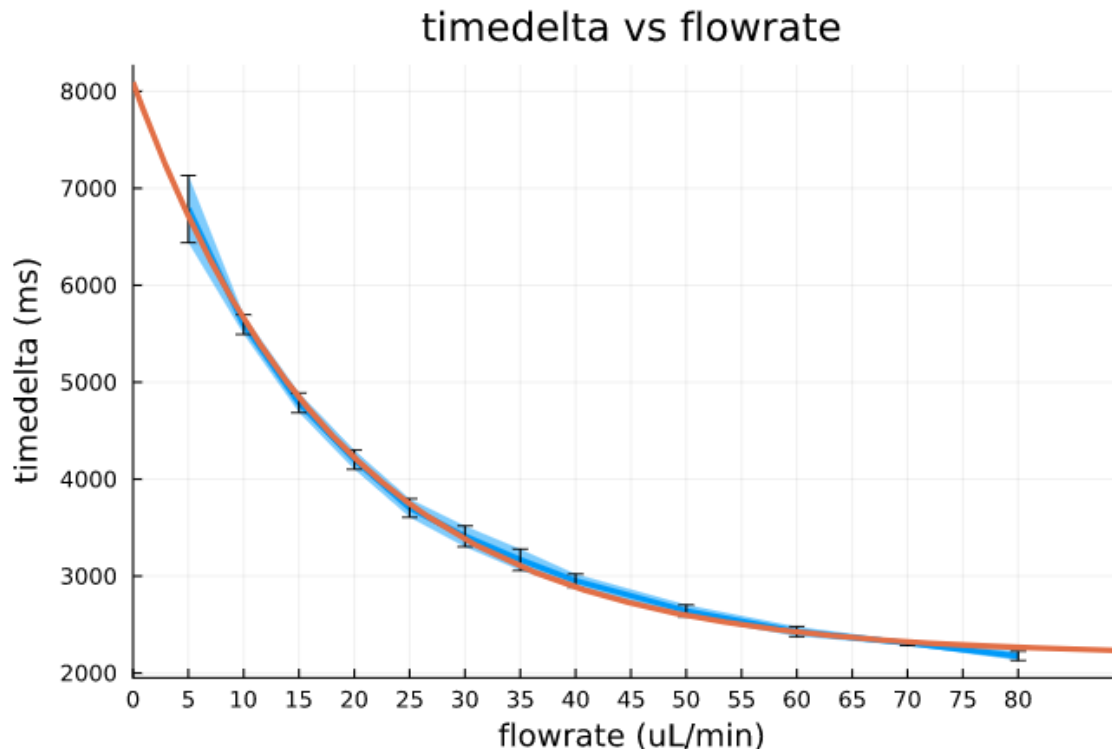


Figure 3.9: Timedelta vs flow rate graph, with a fitted decaying exponential function

The function for the decaying exponential is a 3 parameter model of the form:

$$\tau(v) = A + Be^{-Cv}$$

Where A, B and C are the fitted parameters. We guessed this equation and it seems to fit the data well. After solving for the flow rate we arrive at the following equation which takes timedelta as input and outputs the corresponding flow rate value.

$$v(\tau) = \ln\left[\left(\frac{B}{\tau - A}\right)^{1/C}\right]$$

The fitted parameters A, B and C are fairly consistent across the three flow sensors we tested. However, they do differ slightly due to the small differences in the geometry of the measurement tube. Calibration should be done for each sensor to take these differences into account. Once the parameters are fitted for that specific sensor, they are hardcoded into the sensor's flash memory. Since the parameters should depend only on the geometry of the sensor, they should not change for the remainder of the sensor's lifetime.

3.3.3. Firmware Details & Cyclic Executive

To reduce the amount of memory and compute time required, we only take 13 temperature measurements with each measurement spaced 1 second apart. Then we use a plain C implementation of the Levenberg-Marquardt algorithm to perform a non-linear least squares fit of the analytical model to the temperature data [5]. Then, we use the fitted parameters to calculate our timedelta.

The analytical model is a 5 parameter model. Our initial guess vector is $p = [q, v, d, k, a] = [30, 0.5, 1, 0.598, 0.143]$. We use the thermal conductivity of water, thermal diffusivity of water and a signal strength of 30C as our initial guess. The velocity and delay factors are experimentally determined as a part of the calibration process. Heater-sensor distance, x , is a fixed value and it is set at 3 mm for sensor #1 and 5 mm for sensor #2.

Experiments show that this initial guess vector converges for all flow rates between 1.00 uL/min and 80.00 uL/min. It does not converge if there is no flow or if the flow rate is too high. If none of the temperature data points are above some minimum threshold (0.3 C), then we output 0.00 uL/min. If there is, and the algorithm still fails to converge, we output "OOR" for out of range as we assume the flow rate is much higher than 80 uL/min. This is enough to satisfy FS2.

For simplicity, the firmware is implemented as a cyclic executive. The flowchart in figure 3.10. We also set the maximum allowed iterations for the Levenberg-Marquardt algorithm so that we would get a flow rate reading exactly once every 15 seconds.

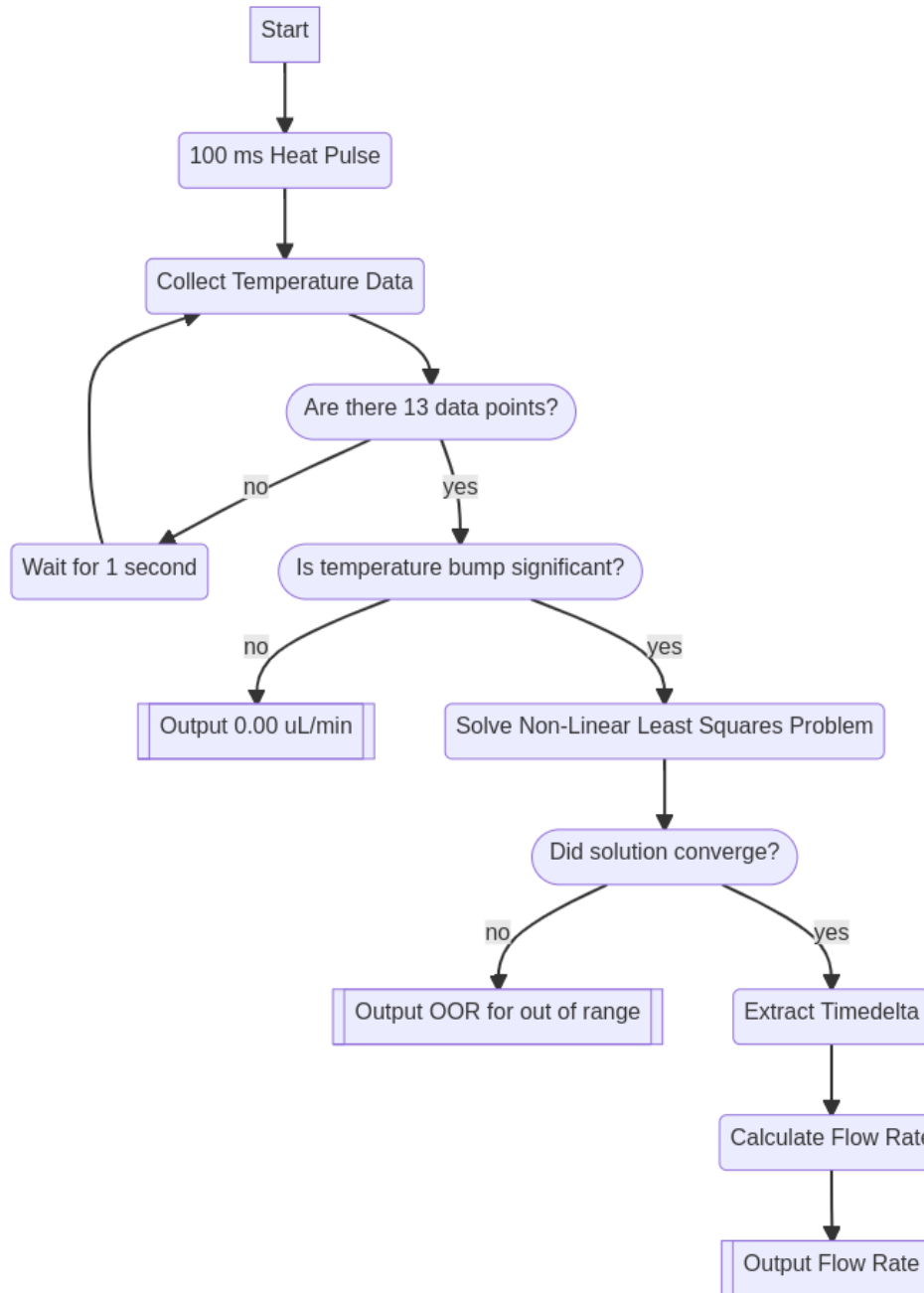


Figure 3.10: Flow rate sensor firmware flowchart

3.4. Manufacturing Guide

The PCB is made through standard PCB manufacturing and PCB assembly techniques. As such, they will not be covered in this guide.

To make the measurement tube, we need the following tubing sections:

Number of Sections Required	Tubing Sections
5	3mm stainless steel tube
3	3mm tygon tube
1	8.5mm tygon tube
1	tygon tube carrying reagent into the sensor
1	tygon tube carrying the reagent out of the sensor

Table 3.3. Required tubing sections to construct the measurement tube

Tygon tubing is flexible so they can be cut with scissors or wire cutters.

The stainless steel tubing sections are cut from 29G insulin needles. Using scissors or wire cutters would permanently deform the tube and hinder measurement accuracy.

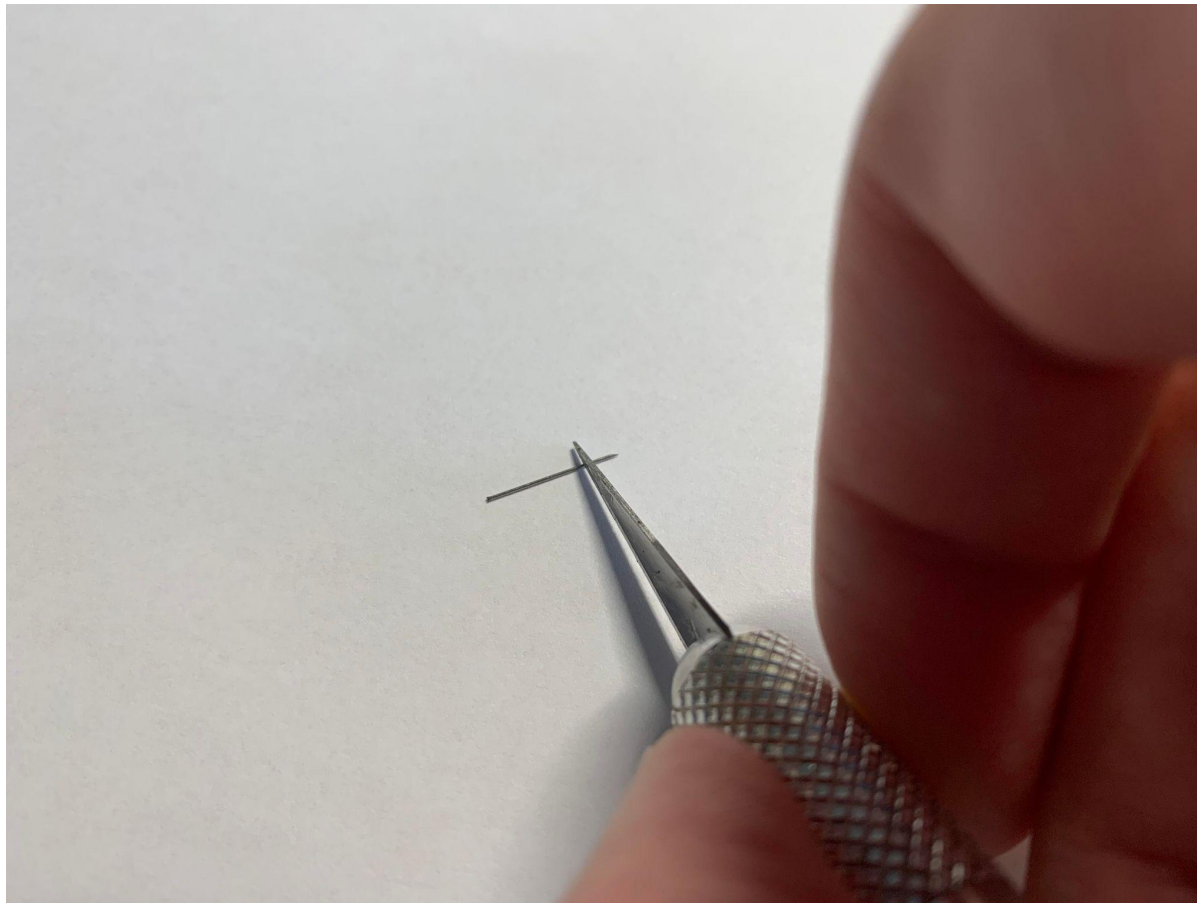


Figure 3.11: To make a clean cut of the stainless steel tubing, gently apply some downward force and roll the needle to create a v-groove before snapping the tube in two

As shown in figure 3.11., to cut the insulin needle without deforming the tube, use a scalpel blade. First use a wire cutter to detach the needle from the luer lock. This allows the needle to roll smoothly on the table. Gently apply some force with the scalpel blade and roll the needle back and forth to create a v-groove. Once there is sufficient grooving, take a needle nose plier and break off the

stainless steel section. The stainless steel sections should be cut from the middle of the needle. Avoid using the sharp end or the luer lock end of the needle as a stainless steel section.

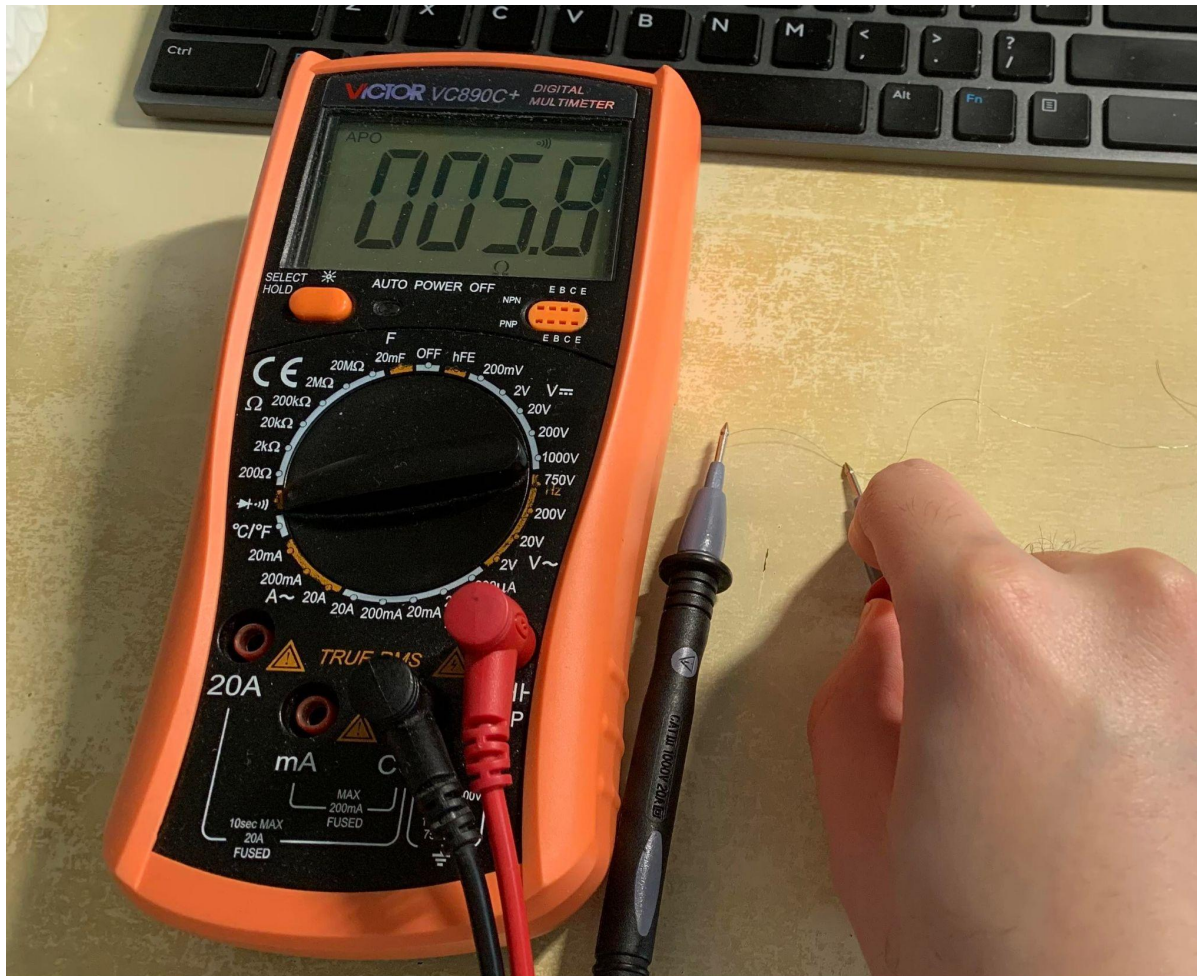


Figure 3.12: Attach one end of the heater wire to a multimeter probe and sweep the other until 6 ohms of resistance is measured. This is the length of the heater wire for the sensor.

Measure around 6 ohms of heater wire with a multimeter as demonstrated in figure 3.12.

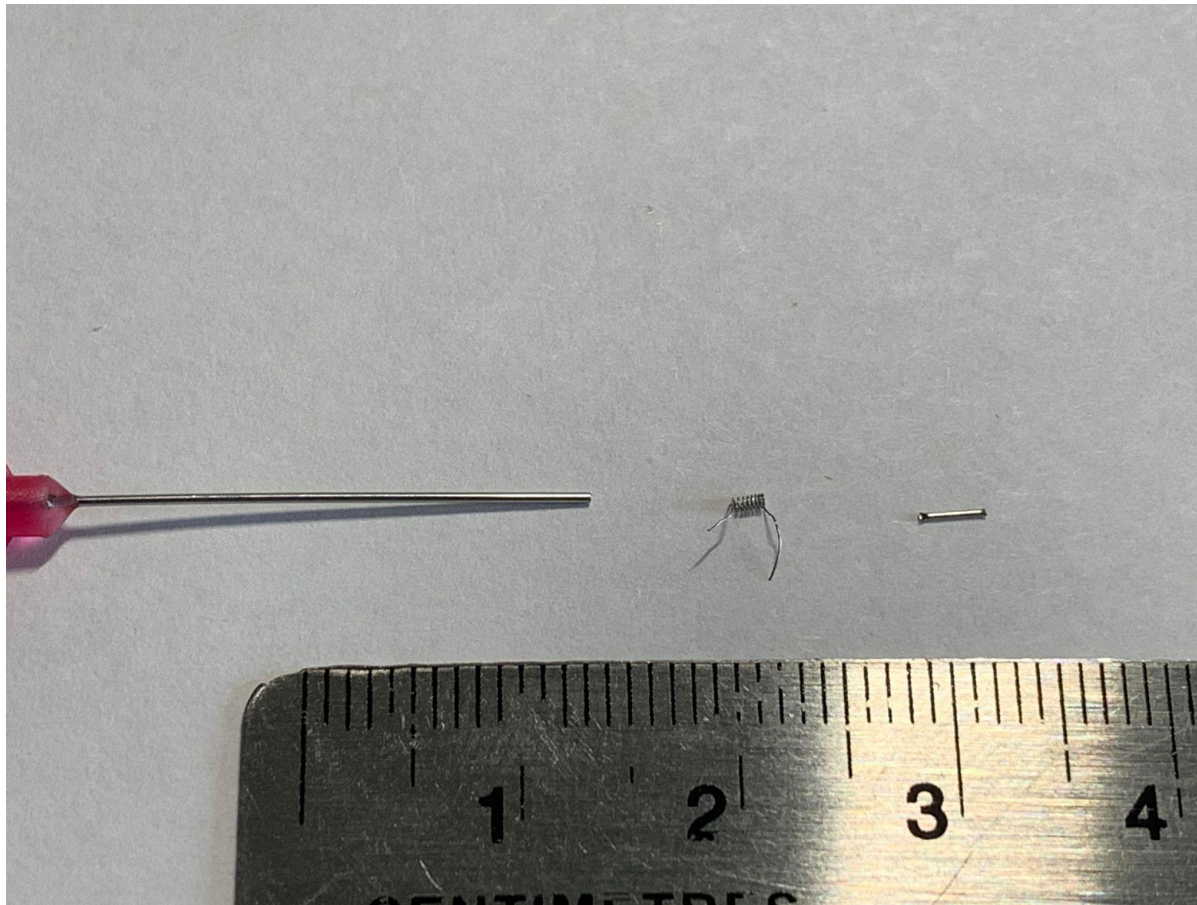


Figure 3.13: Going from left to right, the 23G syringe around which we wound the heater wire, the resulting heater coil and the 29G stainless steel tube which will slip in the heater coil

Wound the heater wire around a 23G syringe. Remove the wounded heater coil from the 23G syringe and slip it on a stainless steel section. The resulting components are shown in figure 3.13.

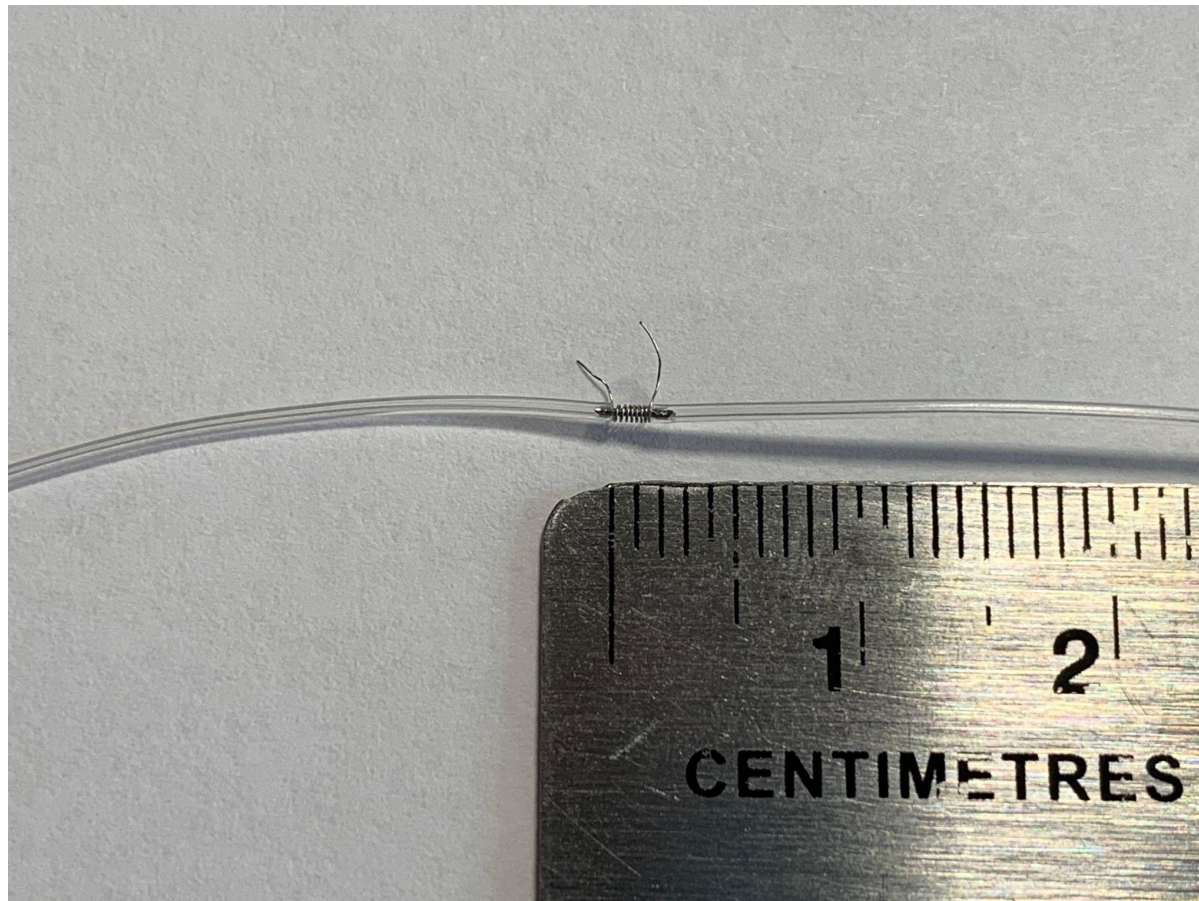


Figure 3.14: Heater section joining the input and output tygon tubes

Insert the stainless steel section into the heater coil and push both ends into the tygon tubing as shown in figure 3.14. Leave at least 0.5 mm overlap to ensure mechanical integrity. Repeat this process with the rest of the tubing sections until the measurement tube looks like figure 3.6.

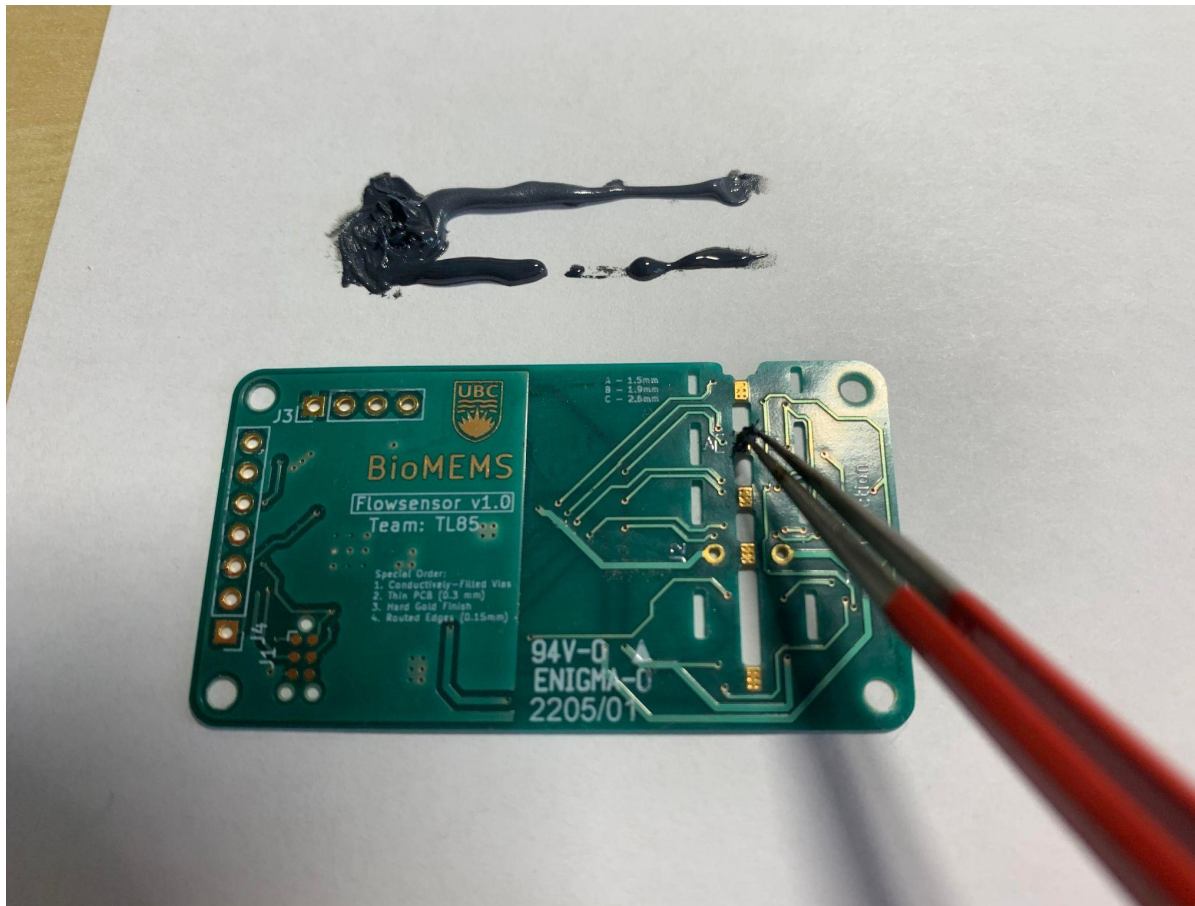


Figure 3.15: Mixing the thermally conductive adhesive and applying it on the sensor pads

To adhere the measurement tube to the PCB, squeeze a few centimeters of thermally conductive adhesive, mix it, then apply it with a tweezer to the sensing pads of the PCB as shown in figure 3.15.

Carefully place the measurement tube on the PCB, making sure that the exposed stainless steel sections land on the thermally conductive adhesive, thereby thermally coupling the sensing pads with the stainless steel sections.

Let the sensor sit for 24 hours at room temperature to allow the thermally conductive adhesive to cure.

3.5. Calibration Guide

Manual calibration is required. Here are the resources required for the calibration step.

1. STLINK-V3
2. Access to the github repo https://github.com/jackyruth/Low_Cost_Microfluidic_Flowsensor.git
3. A system to drive a reference flow rate

Here are the steps to calibrate the sensor

1. Connect the STLINK-V3 to the sensor, see the product specification sheet for the sensor pinout diagram
2. Program 'stm32/data_collection' firmware
3. Drive a constant flow rate through the sensor and store the data. Preferably, the collected data corresponds to flow rates between 5 uL/min and 80 uL/min in increments of 5 uL/min
4. Push the data through 'julia/flowrate_detection.jl' which outputs three calibration constants A, B and C
5. Change the calibration constants in 'julia/functional_firmware'

Program the 'julia/functional_firmware' and the device should start returning proper flow rate measurements.

3.6. Robustness to Varying Operating Conditions

3.6.1. Temperature Variance

In theory, the thermal time-of-flight flow sensing technique is robust over a wide range of reagent and ambient temperatures. Using the idealized model, which accurately describes the situation due to how well it fits the data, we can tell a few things about the sensor's performance over varying temperatures.

$$T(x, t) = \frac{q_0}{4\pi k t} e^{\left[-\frac{(x-vt)^2}{4at} \right]}$$

Figure 3.16: Analytical model of the temperature curve

Since we are only interested in the timedelta which is $\text{argmax } T(t)$, we can see that the heat signal strength q_0 , which is the difference between the temperature of the heater and the temperature of the reagent, has no effect on the timedelta. Furthermore, the nichrome heater wire heats up to the proper temperature almost instantaneously in comparison to the time it takes to perform a measurement. This gives us the confidence that as long as there is a detectable change in reagent temperature, then the timedelta will be constant in a vast range of ambient and reagent temperatures (FS5 & FS6).

3.6.2. Reagent Variance

Different reagents have varying thermal conductivity k and thermal diffusivity a . Although they are set to the default value for water at 20C initially, they are actually some of the parameters we perform the non-linear least squares fit with. Therefore, we expect the performance of the sensor to be fairly consistent across a variety of reagents (FS4).

3.7. Known Issues & Future Improvements

3.7.1. PCB Self Heating

Due to the thinness of the PCB, heat can be carried from the heater wires to the temperature sensor through the PCB substrate instead of through the measurement tube. This spoofs a flow rate of around 4 uL/min even when the reagent is not flowing.

This phenomenon introduces error when measuring low flow rates. If this was not a problem, we expect the error to continue decreasing linearly with the flow rate instead of having a minimum absolute error of 4 $\mu\text{L}/\text{min}$ which is what it has now.

One approach to solve this problem in future iterations is to make the flowsensor with two PCBs instead of one. This will allow us to thermally insulate the PCB hosting the heater from the PCB hosting the sensors such that the only path for thermal transfer is through the measurement tube.

If we succeed, and the measurement error will decrease linearly with flow rate, then we can intuitively characterize the sensor accuracy as % of measured value instead of % of full scale.

However, even if we do succeed, we can not measure arbitrarily small flow rates. Eventually, it will take so long for the heated reagent to arrive at the temperature sensor that the thermal diffusivity of the reagent would have rendered the temperature peak completely undetectable.

3.7.2. Lower Accuracy at Higher Flow Rates

As figure 3.9 shows, the relationship between the timedelta and the flow rate is an exponential decay.

The faster the flow rate, the harder it is to distinguish them from the timedelta. Eventually, the noise in the measurements would dominate.

There is a simple way to increase the accuracy of the sensor at higher flow rates using the existing hardware. The current firmware only makes use of the sensor closest to the heater. The firmware can be enhanced to detect that the flow rate is high and use temperature data from a sensor that is further away to yield the flow rate measurement.

This would shift the exponential decay curve in figure 3.9 into the higher flow rate region where it would accurately measure up to 80 $\mu\text{L}/\text{min}$ and only start to increase in flow rate error at around 100 $\mu\text{L}/\text{min}$.

3.7.3. High Measurement Latency

The high latency of the sensor, which is measured in seconds, is a result of constructing the sensor out of materials which are directly manipulatable by the human hand.

It takes around 100 ms to heat the reagent, 3 seconds for the heated reagent to travel to the temperature sensor and around 10 seconds for the reagent to cool back down to its initial temperature. Perhaps if active cooling was introduced, then the latency can be decreased down to a minimum of 3 seconds.

The limiting factor is the time it takes the reagent to carry the heat from the heater to the sensor. To shorten this time, either the channel has to be made with a smaller cross section or the distance between the heater and the sensor has to be closer. In either case, making such a sensor requires more advanced manufacturing techniques. Most microfluidic flowsensors are MEMs-based, which increases their cost.

4. Appendix

4.1. Flow Rate Sensor

4.1.1. Overview of Flow Sensing Techniques

A low flow rate restricts the methods of sensing which can be employed. For instance, hall effect sensors require the mechanical turning of a turbine, making it infeasible for microfluidic flow detection. After examining a variety of flow detection methods from this online review [1], the thermal sensing methods are chosen over the mechanical sensing methods for the following reasons:

1. There exist a possibility that thermal sensing methods do not require any microfluidic chip fabrication, making it simpler and faster to prototype
2. Thermal elements and temperature sensors are cheaper than any ultrasonic/optical methods of detection, helping the system to achieve FS-NF6
3. Thermal-electric elements and temperature sensors are generally more reliable than mechanical elements, which follows FS-NF1

Among different thermal sensing techniques [2], time-of-flight sensor is chosen for the following reasons:

1. Time-of-flight sensor uses the delay of the heat transfer rather than the characteristic of the heat transfer, making it possible to achieve FS-NF3
2. Time-of-flight sensor can be made non-invasive as opposed to the hot-wire sensor
3. There are precedence for time-of-flight sensing techniques to achieve FS-F2, FS-F3 and FS-F4

4.1.2. Flow Rate Sensor Prototypes

4.1.2.1. Prototype #1: Temperature Sensing POC

A prototype was made to prove that temperature change can be detected. The following diagram illustrates how the prototype was made.

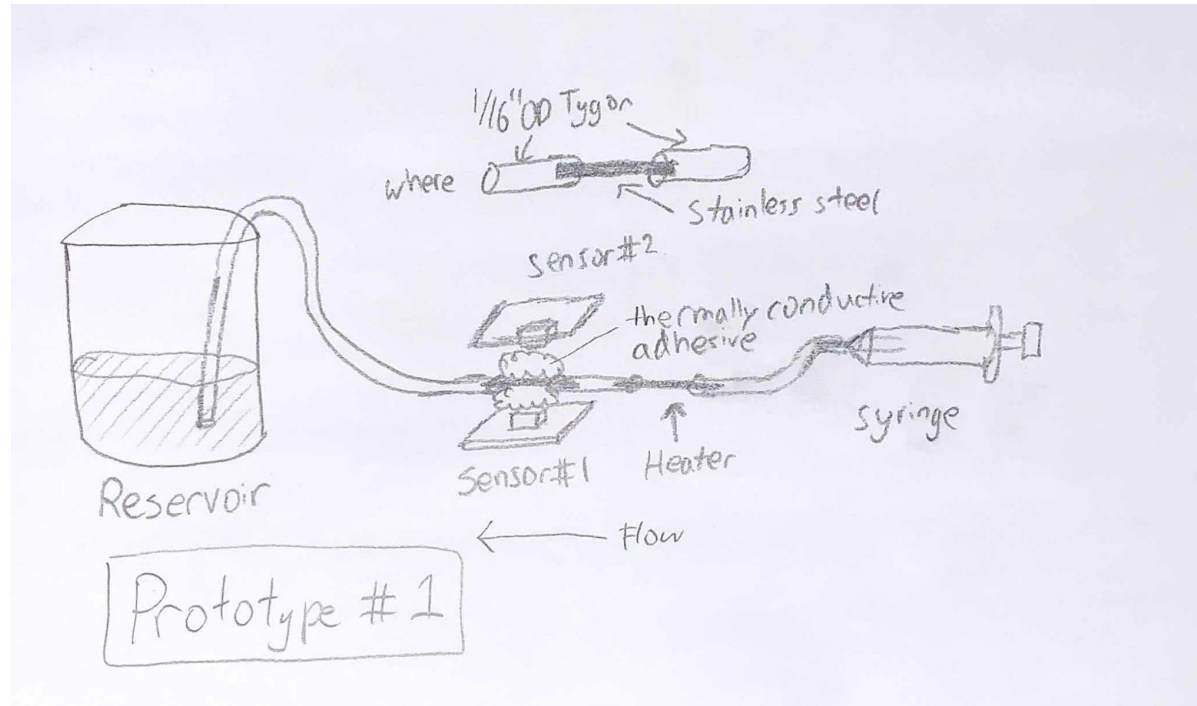


Figure 4.1: Diagram of prototype 1

Two TMP117 high-precision temperature sensors are used [3]. These sensors have an accuracy of 0.1C. They are attached to 1/16"OD microfluidic tubing through the use of thermal adhesives. A live human hand is used as the heater in this proof of concept.

The proof of concept was successful. See the picture below for the temperature bump produced.

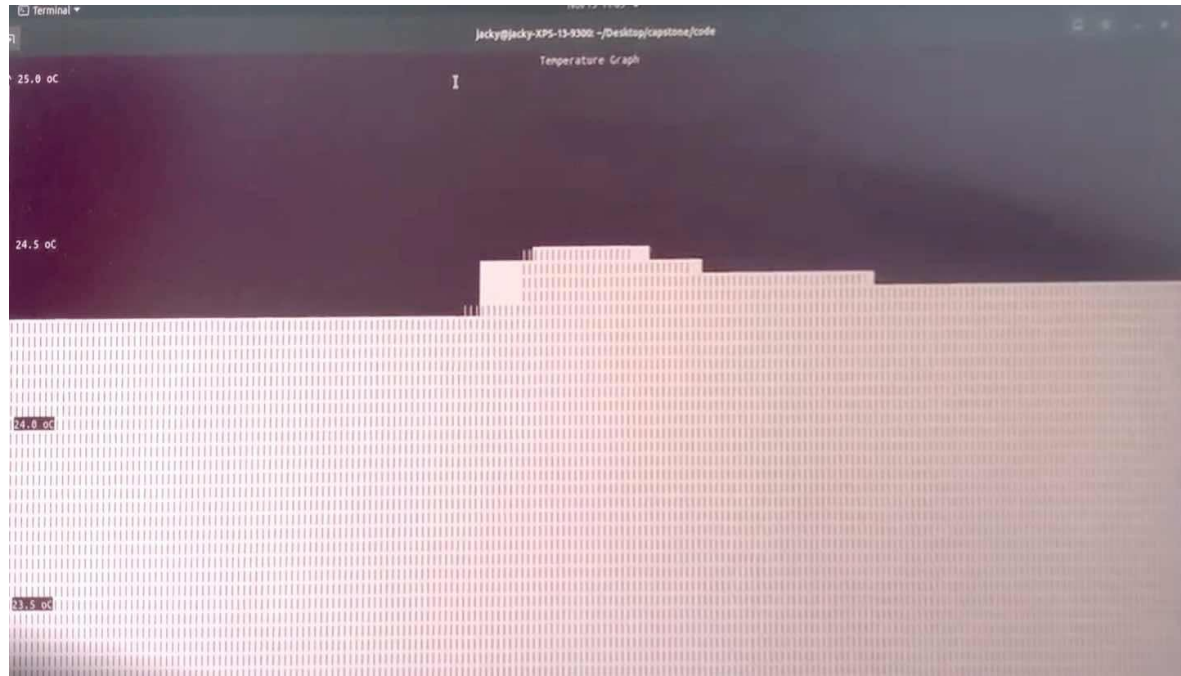


Figure 4.2:Temperature bump as a result of fluid flow

From this result we can see that both sensors (one plotted with “|” and the other with white rectangles) detected a temperature change of around 0.3C.

Since the proof of concept was successful, we are continuing with the thermal time-of-flight sensor.

4.1.2.2. Prototype #2: Thermal Heating/Cooling POC

The goal of this prototype is to prove that we can output a reasonable flow rate measurement with acceptable latency. The primary factors that contribute to increased latency is the time required to heat and cool the fluid. This prototype will demonstrate that we can perform those functions quickly.

The TMP117 will continue to be used as the sensing element. The heating element will be Nichrome wire. It is a resistive wire which we will wound around the stainless steel tubing for maximum conductive heat transfer.

The same thermally conductive epoxy will be used to transfer heat from the nichrome wire to the stainless steel tubing as well as electrically insulate them.

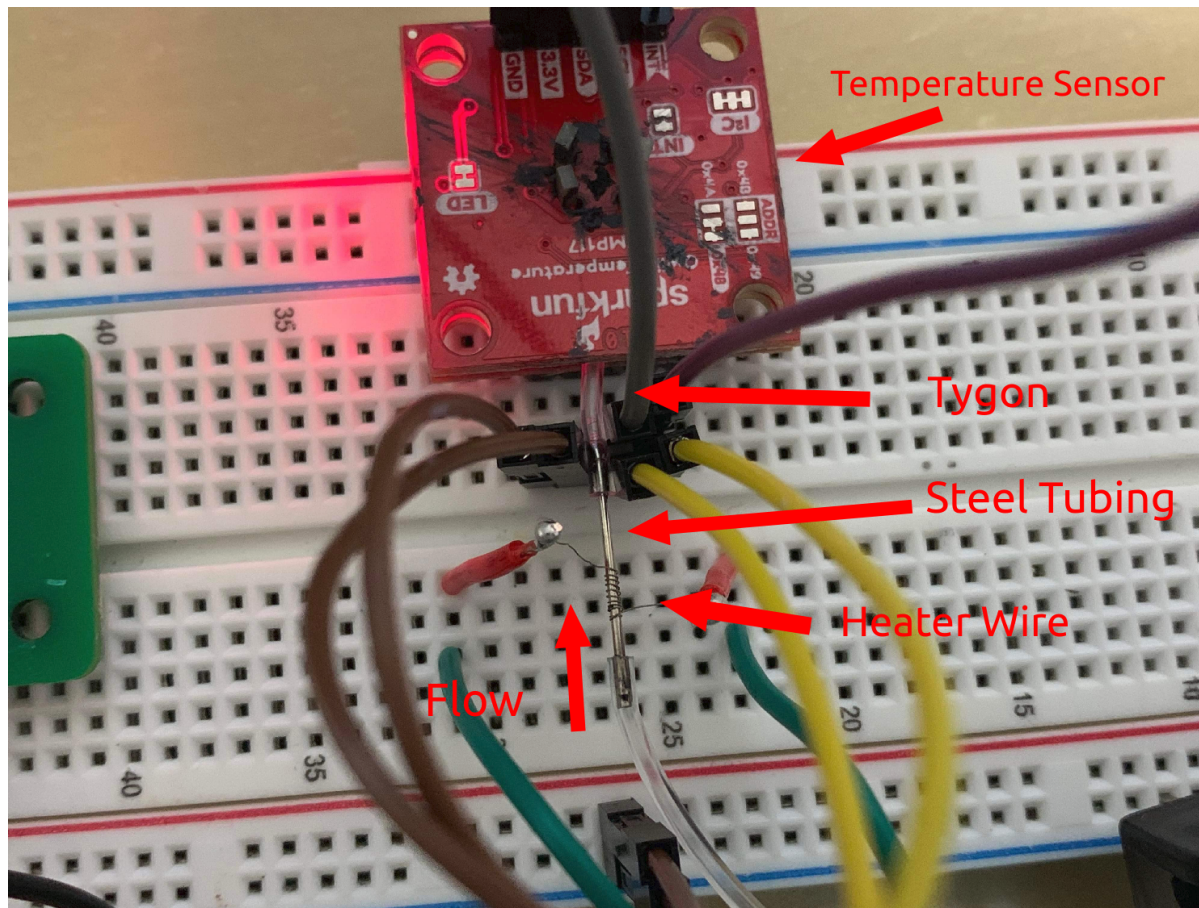


Figure 4.3: Prototype #2, uses nichrome wire as the heating element

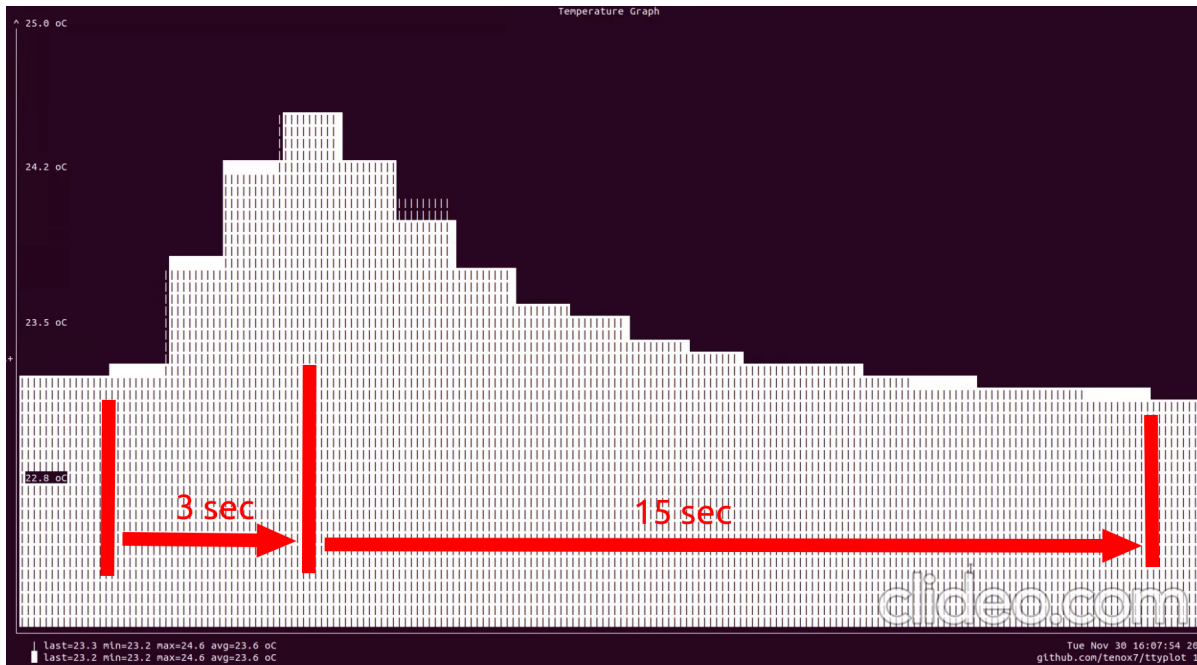


Figure 4.4: Temperature bump with the heater being turned on for 3s and then off by 15 s

Unlike prototype #1, we can actually keep a steady flow rate while detecting the temperature bump caused by the heat carrying fluid.

In figure 9.4, the heater is powered with a pulse for 3s before turning it off for 15s. The sensor senses a temperature change of over 1C. In terms of latency, this means that we can make a measurement every 18 seconds.

This is not ideal, but the next prototype will be able to decrease this latency.

Furthermore, this prototype reveals the complex signal produced by the sensor. It will take theory and experimentation with the heating and sensing signals to produce an accurate flow rate measurement.

Prototype #2 will be used to test different ways of measuring timedeltas. The gained knowledge should carry over to the final product.

4.1.3. BOM Cost Estimation

4.1.3.1. PCB Cost

Different Design in Panel : 1 2 3 4 5 6 e.g.

* Size (single): X mm inch' ↔ mm

* Quantity (single): pcs

Layers: 1 2 4 6 8 10 12 14 16 18 20 22 24 26 28 30

Material: Tg140 FR-4 Tg150 FR-4 Tg170 FR-4 Tg150 FR-4(Halogen-free) Tg170 FR-4(Halogen-free)

High-CTI(>=600V) High-CTI(Halogen-free,>=600V) High Speed(GHz) High Frequency PCBs(DK)

Special Material(High low temperature)

*Tg140 FR-4 Material: Shengyi S1141

Thickness: ≥0.1-0.2 (reviewed) 0.2 0.4 0.6 0.8 1.0 1.2 1.6 2.0 2.4 2.8 3.2 3.6

4.0 4.4 4.8 5.2 5.6 6.0 Other (reviewed) * Unit: mm

Min Track/Spacing: 3/3mil 4/4mil 5/5mil 6/6mil 8/8mil 

Min Hole Size: 0.15mm 0.2mm 0.25mm 0.3mm No Drill 

Solder Mask: Green Red Yellow Blue White Black Pink Grey Orange Transparent Purple Matte black Matte green None

Silkscreen: White Black Yellow Blue Grey None

Edge connector: Yes No

Surface Finish: HASL lead free Immersion gold(ENIG) OSP Hard gold Immersion silver(Ag) Immersion Tin ENEPIG None(Plain copper)

Au/Ni thickness: Au:5U"/Ni:120U" Please choose other options of Gold /Nickel thickness here

Finished Copper: Bare board(0 oz Cu) 0.5 oz Cu 1 oz Cu 2 oz Cu 3 oz Cu 4 oz Cu 5 oz Cu 6 oz Cu 7 oz Cu 8 oz Cu 9 oz Cu 10 oz Cu 11 oz Cu 12 oz Cu 13 oz Cu 

Pricing And Build Time

PCB Detail List

Material	Tg140 FR-4
Ink	TAIYO,Kuangshun
Board type	Single pieces
Layers	2 Layers
Size	6x3 mm
Quantity	500(single)
Thickness	0.2 mm
Min Track/Spacing	3/3mil
Min Hole Size	0.15mm
Solder Mask	Green
Silkscreen	White
Surface Finish	Hard gold
Au:5U"/Ni:120U"	0.5 oz Cu
Finished Copper	via filled with copper;
Additional Options	
Final Inspection Report(free)	Default Inspection Report

PCB Price

Build Time	Qty	Total
<input checked="" type="checkbox"/> 7-8 days	500	\$ 364.43

Final price is subject to our review.

Shipping Cost: US \$29.89

UNITED STATES OF AMERICA DHL 2-4 business days , wt : 0.309 kg

CHN Time Zone(GMT+8): 2022/1/22 5:30:08

Payment before 2022/01/22 06:00 (GMT+8 Only PCB)

Shipment Date 2022/2/23 AM	Delivery Date 2022/2/26
----------------------------	-------------------------

PCB Cost: US \$ 364.43
Stencil Cost: US \$ 10.00
Shipping: US \$ 29.89
Total: **US \$ 404.32**

Figure 4.5: PCB with 0.2 mm thickness, hard gold finish and via filled with copper comes out to be 0.81 USD per PCB from PCBWay

As figure 9.5 shows, even with a special order PCB with a 0.2 mm thickness, hard-gold finish and copper-filled vias, it would only cost 0.81USD per board when we purchase 500 boards from PCBWay.

4.1.3.2. Electrical Components Cost

All electrical components can be bought from Digikey. The BOM is listed in table 9.1. Note that the price listed is in the scale of 500 assemblies. The cost per unit comes out to be 23.64CAD.

Component Name	Quantity	Digikey M/N	Price Per Unit
tmp117	4	296-52215-1-ND	3.82596
10k	5	311-10KLDCT-ND	0.00667
100nF	9	311-1343-1-ND	0.01516
H-Bridge	1	264-TC78H651AFNGET-N D	1.11546
Crystal	1	XC2738CT-ND	0.54
STM32L432KBUx	1	497-16577-ND	6.07750
D_TVS	1	P4SMA13ACT-ND	0.28360
13pF	2	311-3919-1-ND	0.03555
1uF	2	311-1343-1-ND	0.01337
10uF	1	490-6405-1-ND	0.09498
2.2k	2	RMCF0603FT2K20CT-ND	0.00445

Table 4.1: Digikey BOM

4.1.3.3. Mechanical Component Cost

The thermally conductive adhesive [MG Chemicals 8329TCM-6ML Thermal Conductive Adhesive](#) costs 32.25CAD and can make around 15 flow rate sensors. This means that it is around 2CAD per flow rate sensor.

Two syringes are required to make a single flow rate sensor. The syringes from Amazon are [Easy Touch Bag of 20 1cc 29 1/2 inch 100 units](#) cost 26.33CAD for 100 syringes. This means that it would cost around 0.27CAD per flow rate sensor

A roll of [Tygon Microbore tubing, 0.010" x 0.030"OD, 100 ft/roll](#) can make around 380 flow rate sensors. This means it would cost around 0.56CAD per flow rate sensor.

Finally, the resistive heater wire [0.1mm AWG38 Nichrome Resistance Heating Coils Resistor Wire](#), can make around 500 flow rate sensors. This makes it cost around 0.03CAD per flow rate sensor.

In total, it comes out to be around 2.86CAD per flow rate sensor.

5. Bibliography

- [1] T. E. Team, "Microfluidic low-flow liquid flow meters: a review," Elveflow, Jan. 2021, Accessed: Nov. 28, 2021. [Online]. Available: <https://www.elveflow.com/microfluidic-reviews/microfluidic-flow-control/microfluidic-low-flow-liquid-flow-meters-a-review/>
- [2] J. T. W. Kuo, L. Yu, and E. Meng, "Micromachined Thermal Flow Sensors—A Review," *Micromachines*, vol. 3, no. 3, Art. no. 3, Sep. 2012, doi: 10.3390/mi3030550.
- [3] "TMP117 data sheet, product information and support | TI.com." <https://www.ti.com/product/TMP117#order-quality> (accessed Nov. 28, 2021).
- [4] "Precise temperature measurements with the TMP116 ... - ti.com." [Online]. Available: <https://www.ti.com/lit/pdf/snoa986a>. [Accessed: 14-Feb-2022].
- [5] B. Babich, "A simple implementation of the levenberg-marquardt algorithm in plain C," *Github*. [Online]. Available: <https://gist.github.com/rbabich/3539146>. [Accessed: 14-Feb-2022].

6. Changelog

Date (YYYY-MM-DD)	Author	Change
2022-03-29	Jacky Jiang	Initial Release